

UNCLASSIFIED

AD NUMBER
ADB280152
NEW LIMITATION CHANGE
TO Approved for public release, distribution unlimited
FROM Distribution: Further dissemination only as directed by Office of Scientific Research and Development, Washington, DC 20301, 17 NOV 1946, or higher DoD authority.
AUTHORITY
OTS index dtd Jun 1947

THIS PAGE IS UNCLASSIFIED

A-356

c. 1

4 AUG 1958

UNCLASSIFIED

17 Nov 46

Division 2, National Defense Research Committee
of the
Office of Scientific Research and Development

Nov 46

DISTRIBUTION STATEMENT F:

Further dissemination only as directed by

OSRD, Wash., DC 20330

or higher DoD authority.

FINAL REPORT ON SHOCK TUBE, PIEZOELECTRIC GAUGES,

AND RECORDING APPARATUS

TECHNICAL LIBRARY

BLDG. 305

ABERDEEN PROVING GROUND, MD.

STEAP-TL

by

J. C. Fletcher, W. T. Read,
R. G. Stoner, and D. K. Weimer

TECHNICAL INFORMATION BRANCH

OSRD AND RECORDING APPARATUS

ABERDEEN PROVING GROUND

MARYLAND

NDRC Report No. A-356

OSRD Report No. 6321

NDRC
A-356
c. 1

20020412 047

unauthorized person

Copy No. 40

UNCLASSIFIED

UNCLASSIFIED

Classification changed to *Unclassified*
Authority OSRD 6321 Oct 30 5 Dec 46
Sixty & Syner 12/21
8 Sept 48

Division 2, National Defense Research Committee
of the
Office of Scientific Research and Development

FINAL REPORT ON SHOCK TUBE, PIEZOELECTRIC GAUGES,
AND RECORDING APPARATUS

by

J. C. Fletcher, W. T. Read,
R. G. Stoner, and D. K. Weimer

TECHNICAL LIBRARY
BLDG., 305
ABERDEEN PROVING GROUND, MD.
STEAP-TL

NDRC Report No. A-356
OSRD Report No. 6321

This document contains information affecting the national
defense of the United States within the meaning of the
Espionage Act, U.S.C., 50; 31 and 32. Its transmission
or the revelation of its contents in any manner to an
unauthorized person is prohibited by law.

Submitted on November 17, 1946, by

Walker Bleakney
Walker Bleakney
Princeton University

Approved February 1946
for submission to the Committee

E B Wilson Jr
E. Bright Wilson, Jr., Chief
Division 2
Effects of Impact and Explosion

UNCLASSIFIED

UNCLASSIFIED

This report was edited and prepared for duplication by, and is distributed by:

Technical Reports Section
Office of the Chairman, NDRC
Room 3040, Munitions Building
Washington 25, D.C.

Requests from Service personnel for additional copies should be addressed to: . . .

War Department

War Department Liaison Officer
for NDRC
Headquarters, Army Service Forces
The Pentagon
Washington 25, D.C.

Navy Department

Chief of Research and Inventions
Research and Development Division
EXOS, Navy Department
Washington 25, D.C.

UNCLASSIFIED

Preface

The work described in this report is pertinent to War Department Project OD-03, "Study of Shock Waves," and to Navy Department Project NO-283, "Air Blast Measurements."

The work was carried out and reported by Princeton University under Contract OEMsr-260, and this report is one of the final reports under that contract.

Initial distribution of copies

- No. 1 to Office of the Executive Secretary, OSRD
- Nos. 2 to 25 to Liaison Office, OSRD, for
 - Air Ministry (5 copies)
 - Combined Operations (1 copy)
 - Department of Scientific and Industrial Research (1 copy)
 - Ministry of Aircraft Production (2 copies)
 - Ministry of Home Security (1 copy)
 - Ministry of Supply (6 copies)
 - War Office (2 copies)
 - Additional distribution (6 copies)
- No. 26 to Col. W. S. Bowen, Chairman's Office, NDRC
- No. 27 to Explosives Research Laboratory, Bruceton, Pa.
- No. 28 to Division 2 Files, NDRC
- No. 29 to D. P. MacDougall, Member, Division 2, NDRC
- No. 30 to J. von Neumann, Member, Division 2, NDRC
- No. 31 to G. B. Kistiakowsky, Member, Division 8, NDRC
- No. 32 to R. Courant, Consultant, Applied Mathematics Panel, NDRC
- Nos. 33 and 34 to War Department Liaison Officer for NDRC, for
 - War Department Liaison Officer for NDRC (1 copy)
 - E. L. Bowles, Office of the Secretary of War (1 copy)
- Nos. 35 to 43 to Ordnance Department Liaison Officer for NDRC, for
 - Col. S. B. Ritchie (1 copy)
 - Col. I. A. Luke, Ammunition Development Division (1 copy)
 - Col. W. A. Davis, Ammunition Development Division (1 copy)
 - L. R. Littleton, Ammunition Development Division (1 copy)
 - Ballistic Research Laboratory, Aberdeen Proving Ground (1 copy)
 - Ordnance Research and Development Center, Aberdeen Proving Ground (1 copy)
 - Technical Group, Picatinny Arsenal (1 copy)
 - Office of the Ordnance Officer, U.S. Military Academy (2 copies)
- Nos. 44 to 52 to Army Air Forces Liaison Officer for NDRC, for
 - Air Ordnance Officer (1 copy)
 - Th. von Kármán, Scientific Advisory Group (1 copy)
 - President AAF Board, Orlando, Fla. (2 copies)
 - AAF School Library-Req.265, AAF Center, Orlando, Fla. (1 copy)

C O N F I D E N T I A L

- ALS, AAF Proving Ground Command, Eglin Field, Fla. (1 copy)
Proof Division, AAF Proving Ground Command, Eglin Field, Fla. (1 copy)
Operational Research Section, Continental Air Forces (1 copy)
Air Ordnance Officer, European Theater (1 copy)
- No. 53 to Air Technical Service Command, Wright Field, Dayton, Ohio (TSESE-4I)
- No. 54 to Army Ground Forces Liaison Officer for NDRC
- Nos. 55 to 57 to Corps of Engineers Liaison Officer for NDRC, for
Lt. Col. S. B. Smith (1 copy)
Maj. J. L. Bisch, Engineer Board Experiment Station (1 copy)
Engineer Board, Fort Belvoir, Va. (1 copy)
- Nos. 58 to 79 to Office of Research and Inventions, Navy Department, for
Research and Development Division (4 copies)
Advanced Intelligence Center, CinCPac Advanced Headquarters (1 copy)
Head of Department of Ordnance and Gunnery, U.S. Naval Academy (1 copy)
Demolition Research Unit, U.S. Naval Amphibious Training Base, Ft.
Pierce, Fla. (1 copy)
U.S. Naval Ordnance Laboratory (2 copies)
U.S. Naval Ordnance Test Station, Inyokern, Calif. (1 copy)
Comdr. J. Ormondroyd, David Taylor Model Basin (1 copy)
Capt. W. Diehl, Bureau of Aeronautics (1 copy)
Technical Library, Adlf-2, Bureau of Ordnance (1 copy)
Comdr. J. A. E. Hindman, Bureau of Ordnance (1 copy)
Lt. Comdr. S. Brunauer, Bureau of Ordnance (1 copy)
R. J. Seeger, Bureau of Ordnance (1 copy)
S. H. Wollman, Bureau of Ordnance (1 copy)
A. Wertheimer, Bureau of Ordnance (1 copy)
Research and Development Division, Bureau of Ordnance (2 copies)
Comdr. J. M. Fluke, Bureau of Ships (1 copy)
Comdr. C. H. Gerlach, Bureau of Ships (1 copy)
- No. 80 to U.S. Naval Research Laboratory
- No. 81 to W. Bleakney, Princeton University
- Nos. 82 and 83 to Naval Ordnance Officer, UERL, Woods Hole Oceanographic
Institution

CONTENTS

	<u>Page</u>
Abstract	1
INTRODUCTION	2
<u>Part</u>	
I. DESIGN AND THEORY OF THE BLAST TUBE	4
1. Tube design	4
2. Tube theory	21
II. TECHNIQUE AND RESULTS OF VELOCITY MEASUREMENTS	25
1. Velocity techniques	25
2. Discussion of velocity results	26
III. PIEZOELECTRIC GAUGES, ELECTRONIC APPARATUS, AND OTHER EQUIPMENT.	39
1. Characteristics of flush and wafer quartz gauges	39
2. Response of tourmaline gauges	50
3. Electronic apparatus	59
4. Other equipment	68

List of Figures

<u>Figure</u>	<u>Page</u>
1. Shock tube assembly	5
2. Pressure section of blast tube	7
3. Expansion chamber of blast tube with contactor	9
4. Port section of expansion chamber	11
5. Tube clamps	13
6. Open tube clamps prior to insertion of cellophane	15
7. Cellophane under pressure	15
8. Shattered diaphragm	15
9. Gauge port section and reflecting end plate	17
10. Tourmaline gauge mountings	17
11. Tourmaline gauge mount	18
12. Velocity section	27
13. Velocity unit in place	28
14. Schlieren pulse of shock passing light screen	28

<u>Figure</u>		<u>Page</u>
15.	Percentage deviation from theoretical shock-wave pressure versus chamber pressure	31
16.	Shock-wave pressure versus compression-chamber pressure in blast tube	32
17.	Type "S" gauge assembly with waterproof cable housing	41
18.	Assembled type "S" gauge	41
19.	Section through assembly of Mark 4 crystal gauge. Type "S"	42
20.	Section through assembly of Mark 6 crystal gauge. Type "R"	42
21.	Gauge constant variations	43
22.	Wafer crystal gauge	44
23-25.	Wafer gauge assembly	47
26.	Linearity test of two wafer gauges	48
27.	Temperature effect on quartz wafer gauge	51
28.	Cutaway view of tourmaline gauge construction. Central brass-tab gauge	53
29,30.	Typical tourmaline gauge traces, incident shocks	54
31,32.	Typical tourmaline gauge traces, reflected shocks	54
33-36.	Linearity tests -- gauges 973, 1000, 1001, 1003	57,58
37.	Linearity test of flush tourmaline gauge 938	61
38.	Gauge recording station	62
39.	One channel of a 4-channel amplifier	63
40.	Regulated power supply for 4-channel amplifier	64
41.	Calibration and distribution panel for 4-channel single-sweep apparatus	65
42.	Transient oscillograph used with single-sweep apparatus	66
43.	Initial trigger, delay, and calibrating relay	69
44.	Sweep and beam trigger circuits for <u>H</u> and <u>Z</u> axes	70
45.	Timing oscillator for single-sweep apparatus	71
46.	Firing circuit for use with single-sweep apparatus	72
47.	Film-reading box	73
48.	Multiple manometer	74

FINAL REPORT ON SHOCK TUBE, PIEZOELECTRIC GAUGES,
AND RECORDING APPARATUS

Abstract

The purposes of this report are: (i) to provide a manual covering the design, operation, and calibration of a blast tube for producing shock waves of known pressure-time characteristics, (ii) to review the work done in studying the response of piezoelectric gauges subjected to step-function shocks in a tube, and (iii) to describe the electronic equipment used to record gauge output.

The report consists of an introduction and three parts which contain the following material.

The Introduction gives the background to present tube work in the form of a brief review and summary of an early report by George Reynolds.

Sec. 1 of Part I consists of a description of the present blast tube which represents the final and completely satisfactory results of two years of development. This tube is more easily constructed, holds for greater pressures, and is easier to operate than the original design. The present design, being a great deal heavier, reduces tube vibrations, and the gauges mounted in the tube give much better records.

Sec. 2 of Part I discusses tube theory. In early tube work shock-wave pressures were computed from a simple theory of shock formation. The approximate nature of this theory is discussed. A more accurate method of determining shock pressure is presented in which shock pressures are computed from velocity measurements using the pressure-velocity equation. The validity of this equation for a real gas is discussed and a formula for the effect of humidity is derived.

Sec. 7 of Part II describes the method of measuring velocities with light screens, photocells, and a spiral chronograph. A full discussion is presented of possible sources of error.

Sec. 2 of Part II deals with the results of velocity measurements which are presented in terms of the percentage differences between shock pressures computed from measured velocities and shock pressures predicted by the simple (approximate) theory of shock-wave formation. The pressures computed from velocities vary from 7 to 18 percent below the theoretical pressures over the range of pressures used, which was 3 to 21 lb/in² excess pressure in the shock. In general, the difference increases with pressure and distance down the tube.

Comparison of velocity results obtained at different times and in tubes of different shape and construction agree within 3.3 percent for shock-wave pressures from 3 to 15 lb/in². Effects of thickness of diaphragm, irregularities in tube, extreme differences in room temperature, and other variables

are investigated. It is shown that if a few simple precautions are taken shock-wave pressure will depend only on chamber pressure, so that in further tube experiments and gauge calibration shock pressures may be determined directly from chamber pressures without measuring velocities.

Part III deals with gauge studies and recording apparatus. A description of various types of quartz gauges is given. Apparently erratic variations in sensitivity of quartz gauges were traced to temperature variations. A wafer-type quartz gauge was developed that was not affected by temperature. The sensitivity of many older tourmaline gauges varied with temperature while the sensitivity of the newer tourmaline gauges did not.

The character of records given by tourmaline gauges at various incident and reflected pressures is discussed. It was found that the apparent sensitivity of the gauges decreased as the particle velocity behind the shock wave increased. It is suggested that the gauge disturbs the streamlines and causes a local reduction of pressure. The pressure being measured by the gauge is determined partly by the gauge and is not the pressure that would act at the same point if the gauge were not there.

The third section of Part III describes the electronic apparatus used to record gauge output.

INTRODUCTION

Blast-tube work was begun at Princeton University in 1943 by George T. Reynolds. The early stages of the work were reported by Reynolds^{1/} and subsequent experimentation has been reported in the Division 2 monthly series of AES^{2,3,4/} reports. Although the results of the AES papers will be stated briefly in the various parts of the present report, it is not intended to reproduce here material that has been presented in full elsewhere.

1/ A preliminary study of plane shock waves formed by bursting diaphragms in a tube, by G. T. Reynolds, NDRC Report A-192 (OSRD-1519).

2/ "Pressures behind a shock wave computed from velocity measurements in the blast tube and the correction for humidity," by W. T. Read, included in AES-3 (OSRD-4257).

3/ "Determination of shock-wave pressure in the blast tube as a function of compression-chamber pressure," by W. T. Read, included in AES-5 (OSRD-4514).

4/ "Effect of temperature on gauge calibration," by W. T. Read, included in AES-10 (OSRD-5144).

The following is a brief outline of Reynolds' report by sections:

1. Introduction. An outline of blast-tube history is given with references to both pioneer work and recent reports by Payman and Shepherd^{5,6/}.
2. Apparatus. The essential features of the tube are illustrated and the production of a shock wave by bursting a diaphragm is described. Reference is made to the associated electronic apparatus and its characteristics.^{7/}
3. Theory. (a) A simple theory of the formation of the shock wave is given. From the theory an equation is derived relating shock-wave pressure to compression-chamber pressure.
(b) The reflection of the rarefaction from the closed end of the compression chamber is treated by the theory of adiabatic waves.
4. Procedure and results. A gauge calibrated by a semi-static method gave pressure records in the tube that agreed with the theoretical equation of shock pressure as a function of chamber pressure.

Rarefaction velocities were measured and explained by tube theory and the theory of adiabatic waves.

Methods of eliminating air leakage in quartz gauges are discussed and illustrated by oscillograms.

Since Reynolds' report appeared, advances in tube work have been made along four lines: (i) tube design has been improved; (ii) a more accurate method of determining shock-wave pressure has been developed, in which shock pressures are computed from shock-front velocity measurements; (iii) the studies of gauge response under dynamic loading have been greatly extended; and (iv) improvements have been made in the associated electronic apparatus for recording gauge output. Tube design and the general theory of shock-wave pressure determination are discussed in Part I. The technique and results of velocity measurements are discussed in Part II. Part III deals with piezoelectric gauges and the associated electronic apparatus.

5/ Payman, Proc. Royal Society A 120, 90-109 (1928).

6/ Payman and Shepherd, Paper A.C. 735 Physics/Ex 98.

7/ The measurement of transient stress, displacement and pressure, by C. W. Lampson, NDRC Report A-73 (OSRD-756).

I. DESIGN AND THEORY OF THE BLAST TUBE

1. Tube design

The present calibration tube represents the result of two years of development, during which time a number of designs and variations have been tried. This tube has proved satisfactory throughout a large number of experiments extending from routine gauge calibrations associated with field programs to laboratory studies of shock-wave phenomena by means of piezo-electric gauges. A photograph of the entire tube is shown in Fig. 1. The internal cross section of the tube is a flat-topped circle to facilitate easy mounting of gauges flush with the inside of the tube. Here the tube is set up for a calibration using reflected pressures, that is, the gauges are mounted near the closed end of the expansion chamber. For calibrations using incident pressures, the gauges are mounted nearer to the diaphragm and in general the fore end of the expansion chamber is left open. When incident pressures are used the expansion chamber should extend far enough beyond the gauges to prevent the rarefaction from the open end of the expansion chamber from reaching the gauges before the flat part of the incident wave has passed. This can be accomplished by interchanging the last two sections of the tube in Fig. 1. Since the sections are bolted together this can be done readily; in fact the tube is designed so that several different lengths of expansion and compression chamber can be obtained by proper combination of individual sections.

Figure 2 is a drawing of the knife section of the compression chamber (the second section of the tube in Fig. 1). Figure 3 is a drawing of the 3-ft expansion-chamber section containing the contactor for initiating the horizontal sweep of the cathode-ray oscillograph (the third section of the tube in Fig. 1). Figure 4 is a drawing of the port or gauge section (the last section of the tube in Fig. 1). The first and fourth sections of the tube in Fig. 1 may be used in either the compression or expansion chambers. They are respectively 3 and 6 ft in length. Figure 5 is a drawing of the clamps. These make it possible to change the cellophane diaphragm between shots with ease and rapidity. The end plate of the tube is also held by a similar set of clamps so that it may be quickly removed between shots for

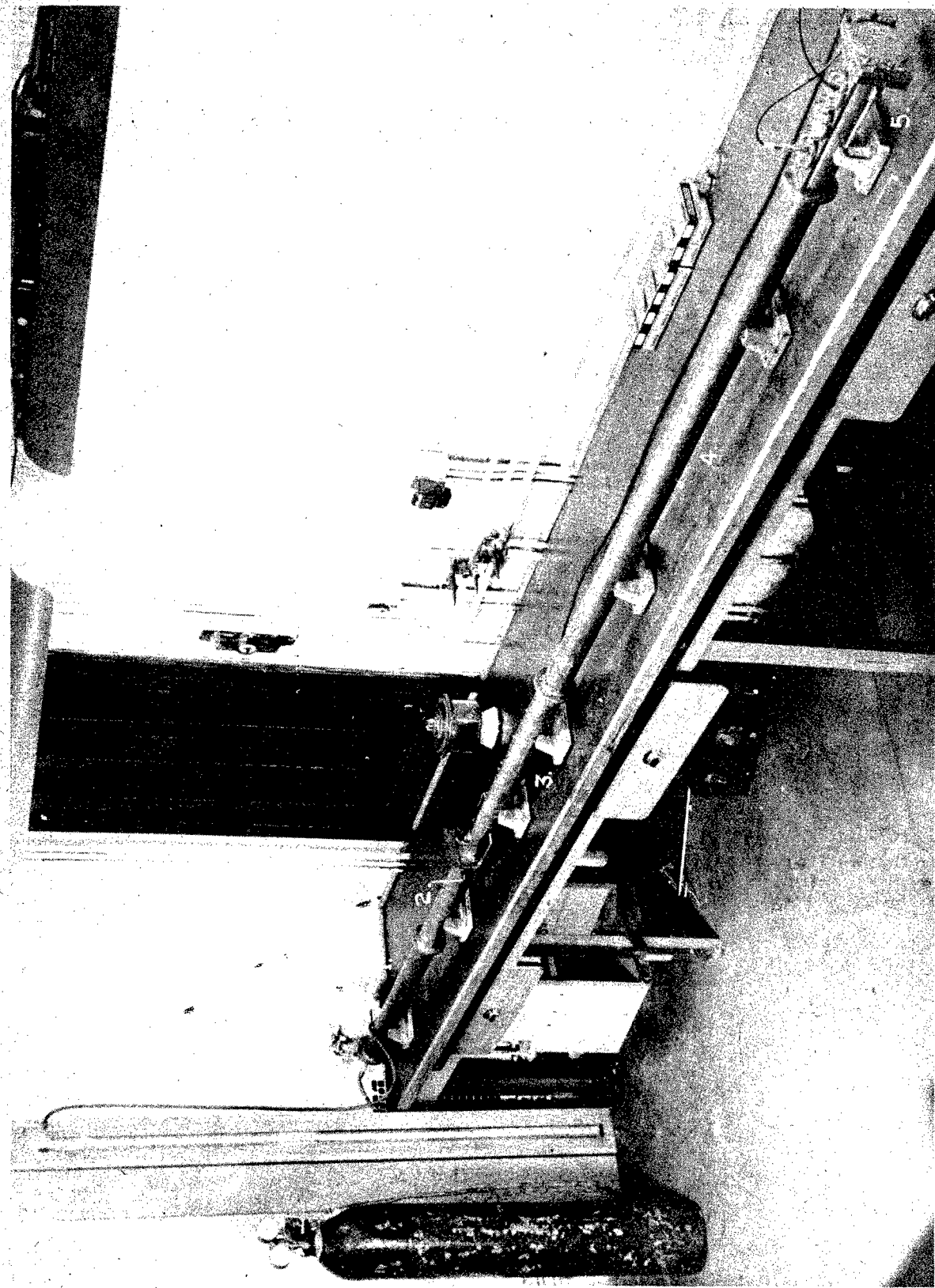
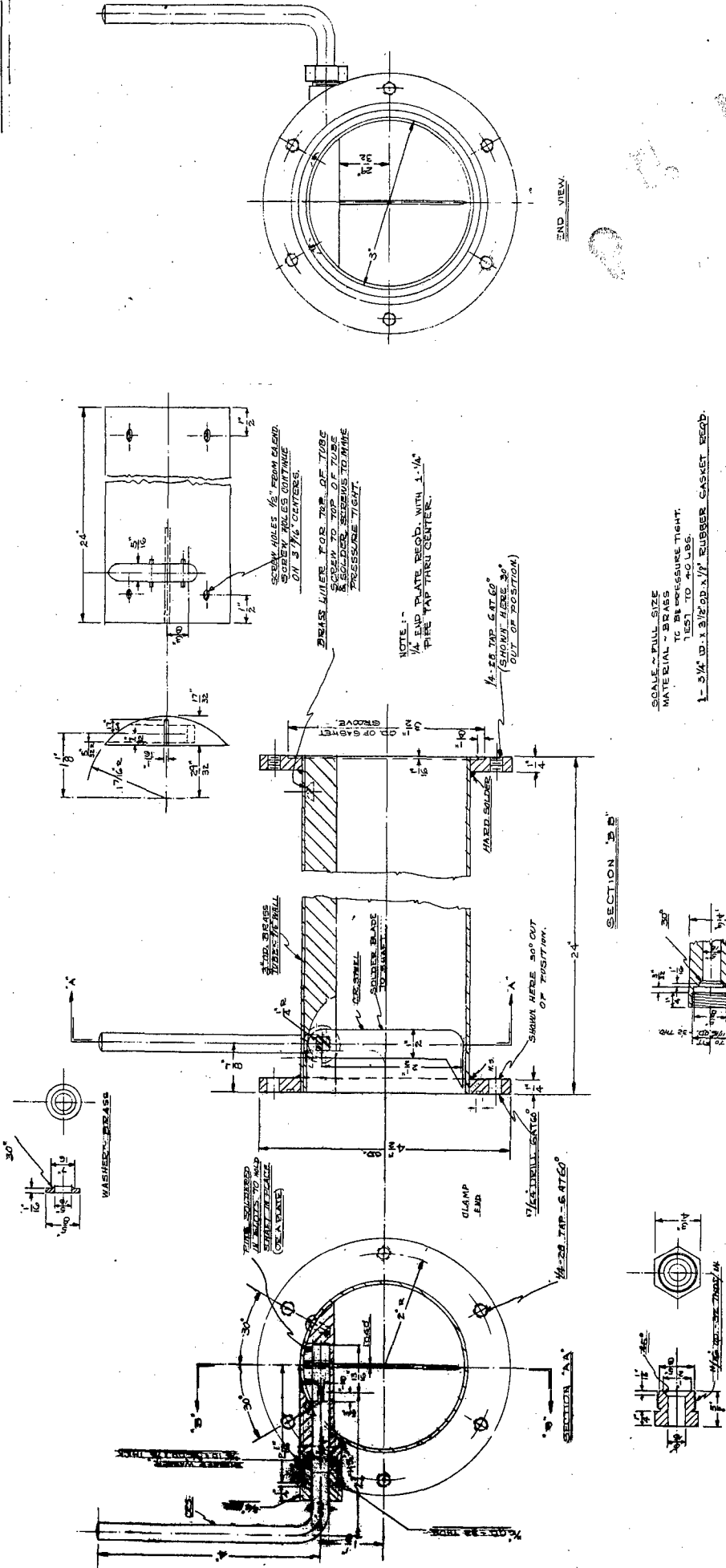


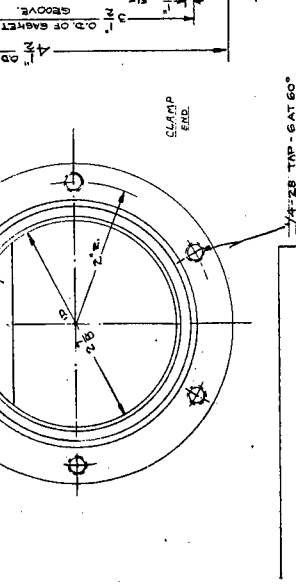
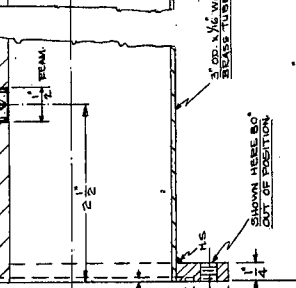
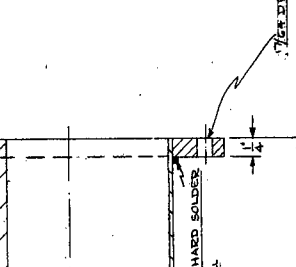
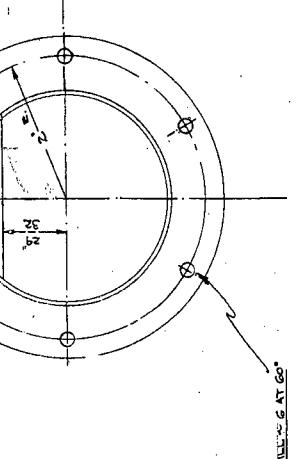
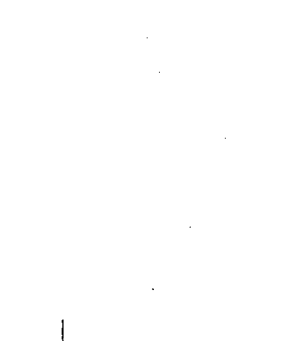
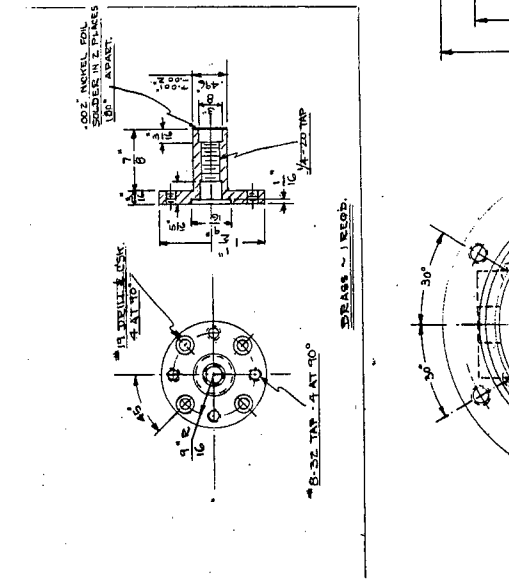
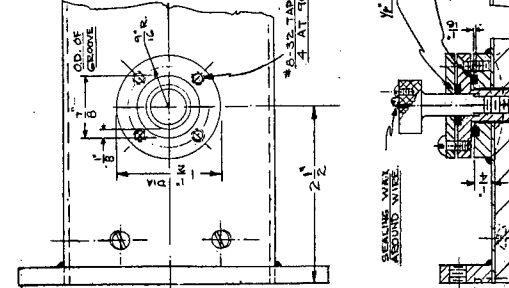
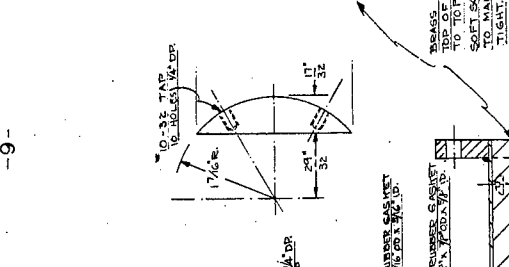
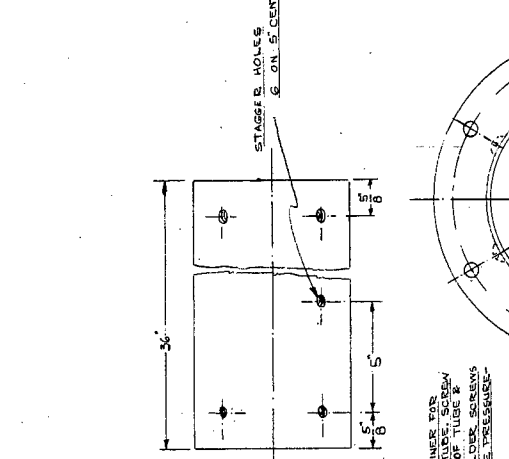
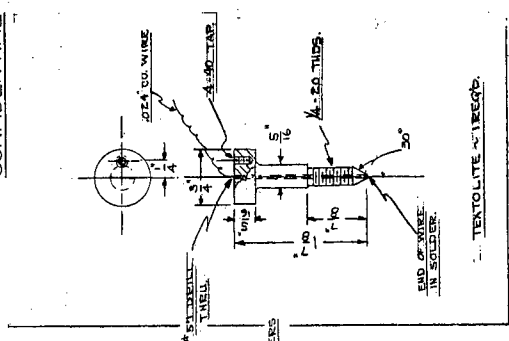
Fig. 1. Shock-tube assembly.



SCALE - FULL SIZE
MATERIAL - BRASS
ALL MOUNTING PARTS
TO BE TIGHT
1 - 3/4" W. X 3/8" D. X 1/4" RUBBER GASKET BEAD.

FIG. 2. PRESSURE SECTION OF BLAST TUBE.

CONFIDENTIAL



9

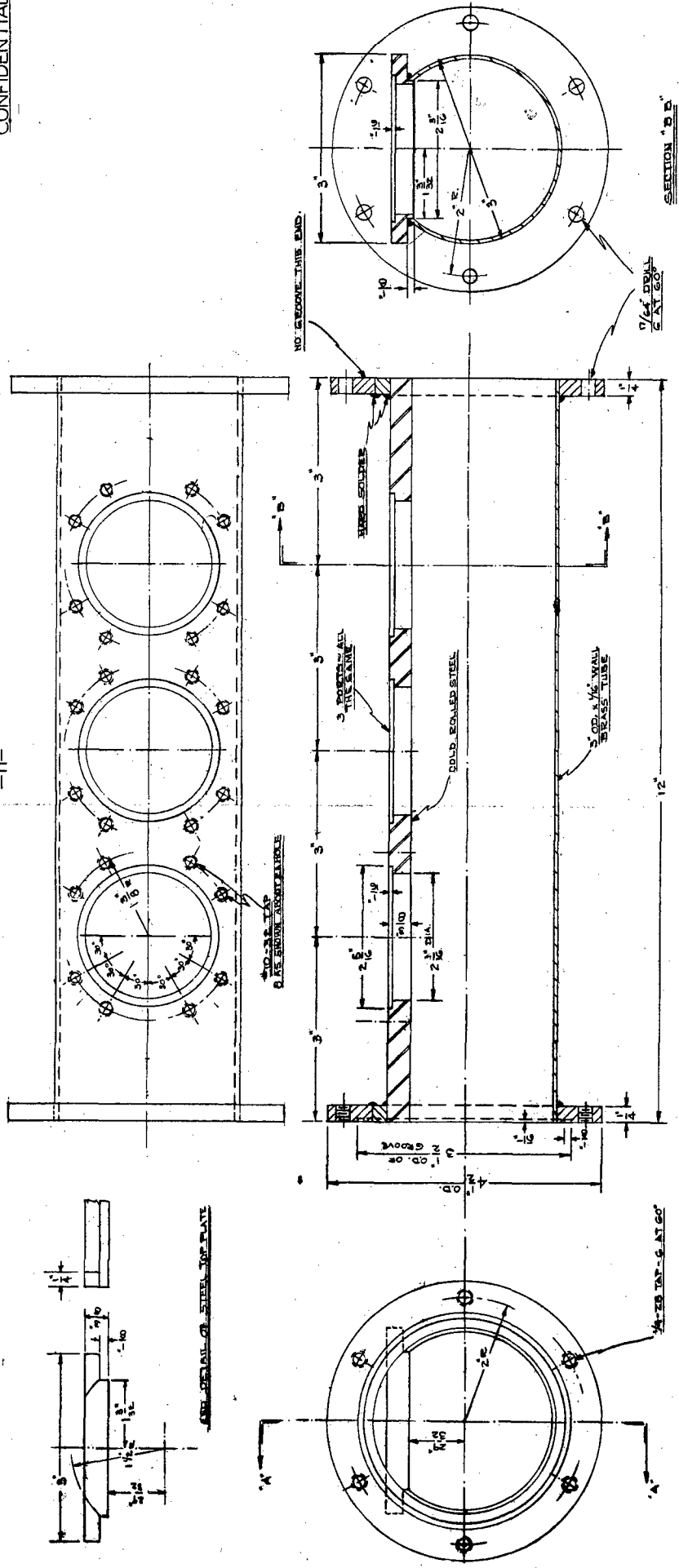
CONFIDENTIAL

FIG. 3. EXPANSION CHAMBER OF BLAST TUBE WITH CONTACTOR.

MATERIAL ~ BRASS

CONFIDENTIAL

-11-

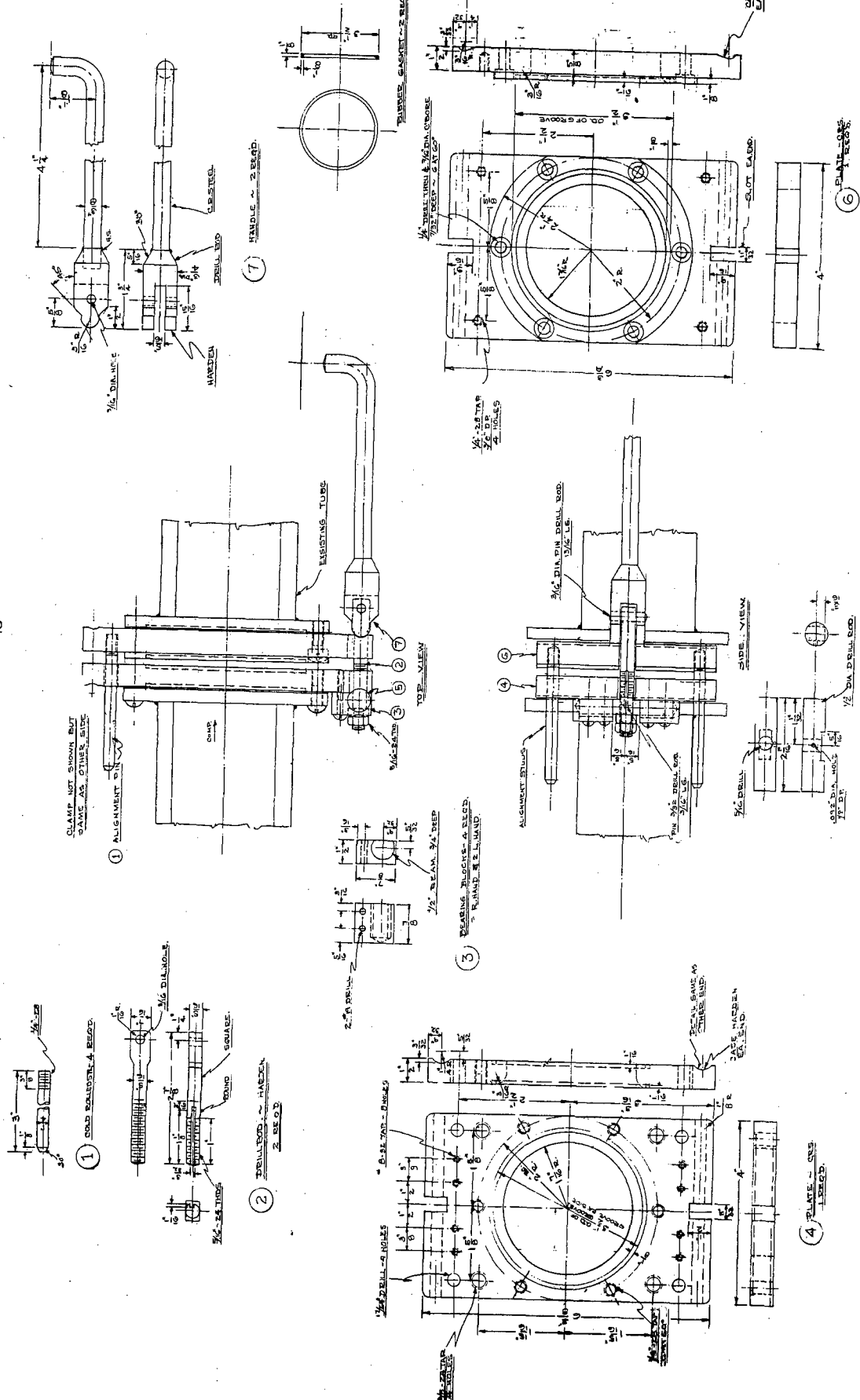


SECTION 'A A'

SECTION 'B B'

FIG. 4. PORT SECTION OF EXPANSION CHAMBER

CONFIDENTIAL



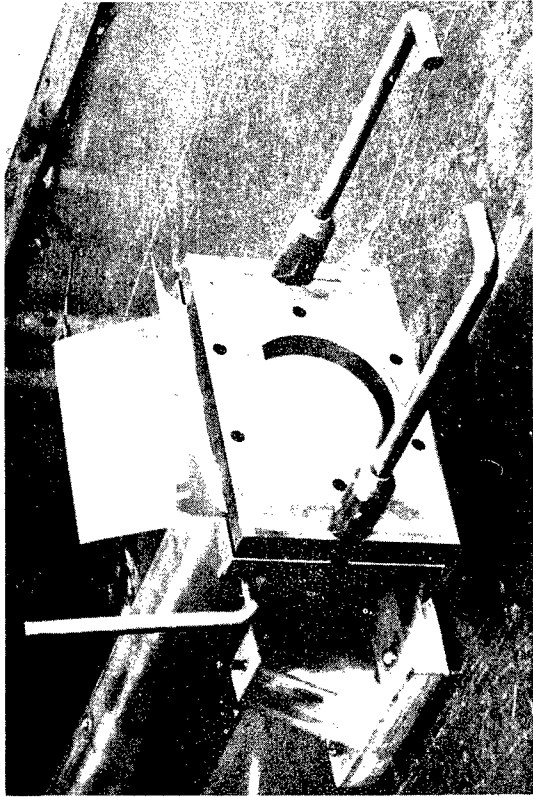


FIG. 7.

FIG. 6. OPEN TUBE CLAMPS PRIOR TO INSERTION OF CELLOPHANE.

FIG. 7. CELLOPHANE UNDER PRESSURE.

FIG. 8. SHATTERED DIAPHRAGM.

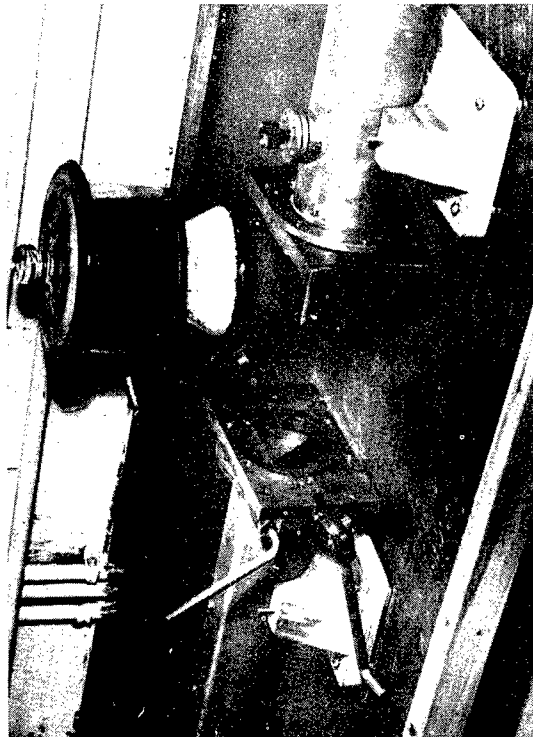


FIG. 6.

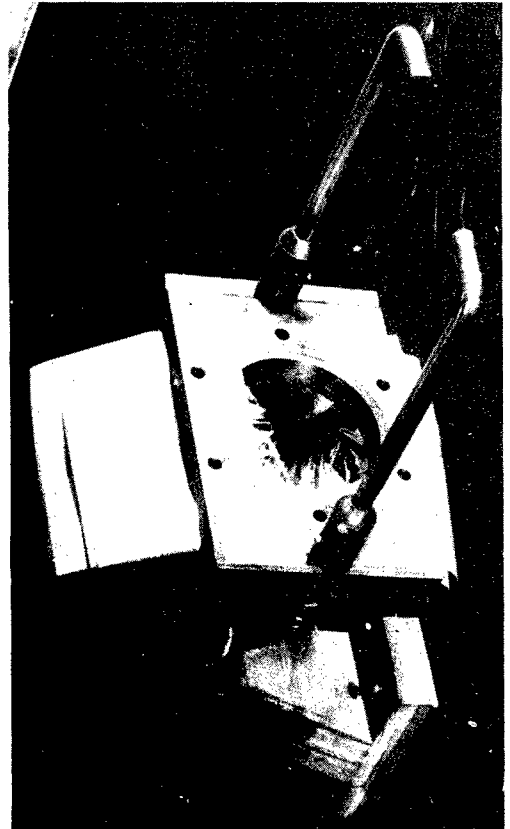


FIG. 8.

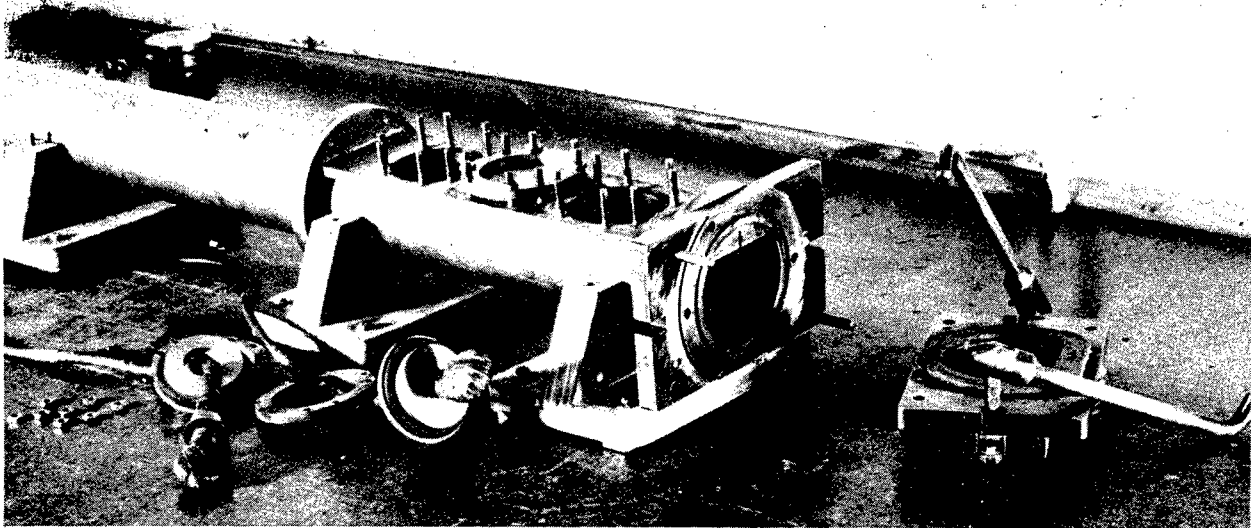


Fig. 9. Gauge port section and reflecting end plate.

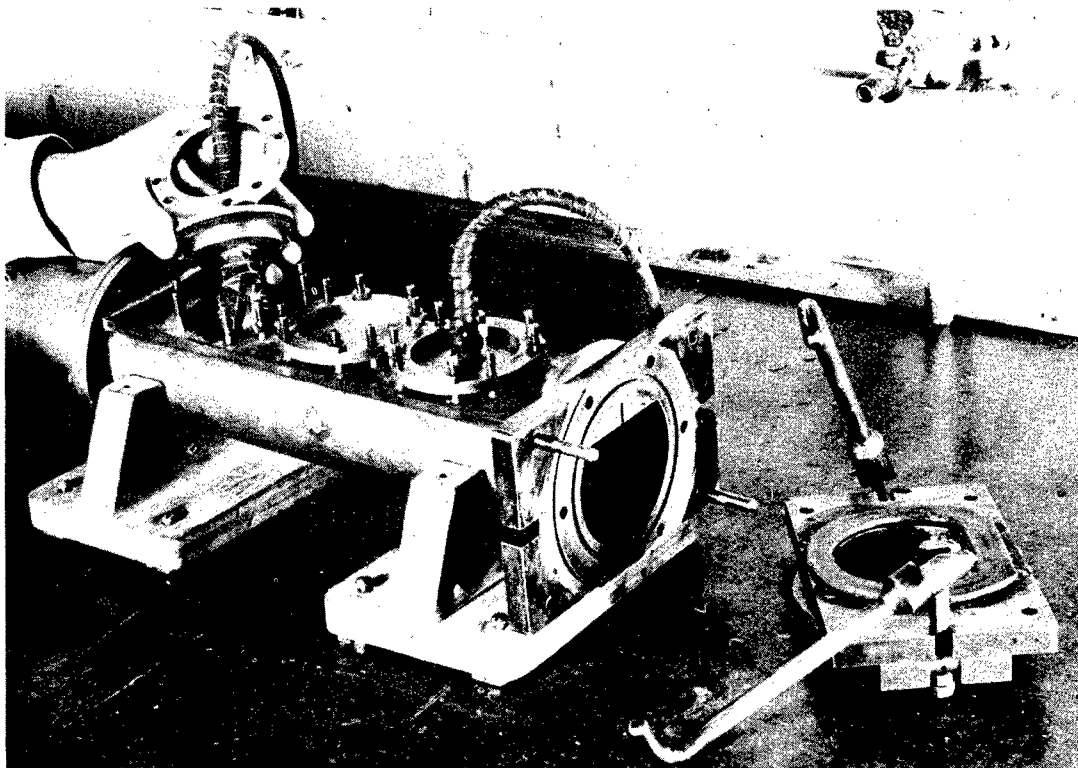
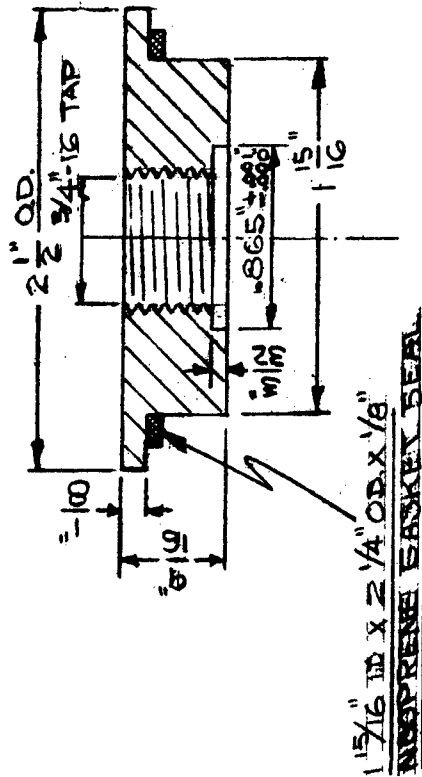
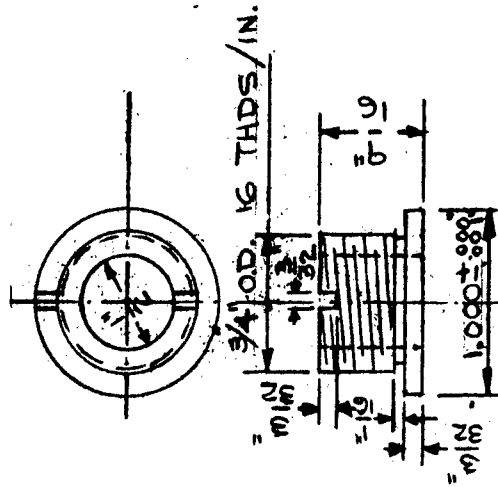
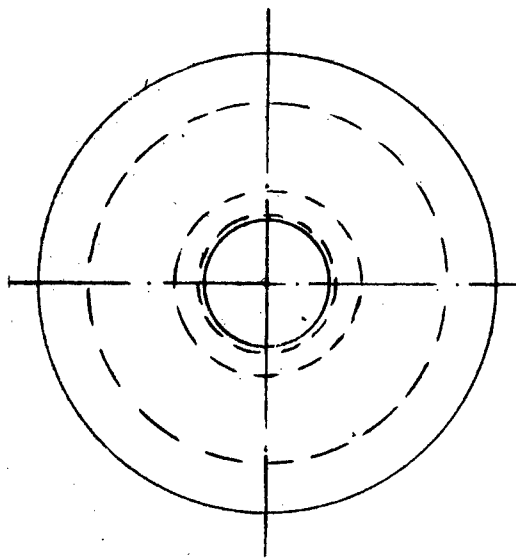
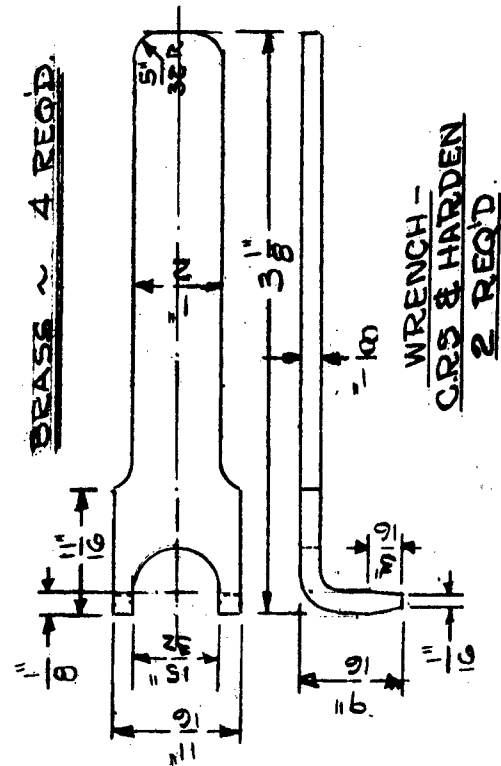


Fig. 10. Tourmaline gauge mountings.



$1 \frac{5}{16}$ " ID x $2 \frac{1}{4}$ " OD x $\frac{1}{8}$ "
NBR PRENE O-RING 5EAL

BRASS ~ 2 REQ'D.



BRASS ~ 4 REQ'D.

WRENCH -
C.R.S. & HARDEN
2 REQ'D.

Fig. 11. Tourmaline gauge mount.

blowing out the shattered bits of the cellophane scattered throughout the expansion chamber.

Figure 6 shows the two chambers separated for inserting the cellophane diaphragm. Before the shot, the pressure in the compression chamber is raised to the desired value by admitting air from a compressed air tank (Fig. 1) through the reduction valve. In Figs. 7 and 8 the expansion chamber has been disconnected from the clamps to show the cellophane before and after it has been shattered by the knife. Figures 9 and 10 show two Bourdon-line gauges being mounted in the gauge section. A drawing of the mounting, which consists of collars and port plugs, is shown in Fig. 11. Brass screw collars are fitted onto the necks of the gauges with enough rubber tape wrapped around the gauge necks to make a snug fit. These collars are kept on the gauges at all times, and the field mounts of the gauges as well as the port plugs of the shock tube are designed to take this fitting. Thus they may be readily transferred from the field to tube for calibration. Ports in which gauges are not mounted are filled by solid plates similar to the one drawn in Fig. 11 but without the threaded hole in the center.

This blast tube differs from the original one used at Princeton in several features, the most outstanding of which is the much greater strength and massiveness of the new tube. The new design has four definite advantages over the old: (i) the absence of soldered seams in all but the gauge port section greatly reduced the amount of work required in construction; (ii) the seamless walls, together with the improved design of the port section, make it possible to use much higher pressures; (iii) quartz gauges mounted tightly in the new tube give very much better records than in the old tube owing to the added stiffness provided by the heavy steel insert which tends to reduce tube vibrations; (iv) the new position of the knife makes it possible for the knife point to reach the diaphragm regardless of the amount of bulging.

The most satisfactory diaphragm material used to date is a commercial product known as No. 600 MST Red Zip Tape.^{8/} It is the custom at Princeton to use a single sheet of cellophane for pressures up to 25 lb/in² in the compression chamber, two sheets from 25 lb/in² to 40 lb/in², three sheets

^{8/} Made by the Dobeckmun Co., 3301 Monroe Avenue, Cleveland, Ohio.

from 40 lb/in² to 65 lb/in², four sheets from 65 lb/in² to 90 lb/in², and five sheets from 90 lb/in² to 100 lb/in². The present tube has not been used above 100 lb/in² in the compression chamber, but computations from the strength and dimensions of the brass show that pressures up to 350 lb/in² in the chamber would not produce inelastic deformation. The excess shock-wave pressure produced by bursting the diaphragm at this compression-chamber pressure would be around 50 lb/in². If the wave were reflected by closing the end of the compression chamber, the excess pressure behind the reflected wave would be approximately 200 lb/in²; this pressure would cause no inelastic deformation provided steel rather than brass screws were used for fastening the end plate.

To obtain high shock pressures it is advantageous to use reflected waves rather than incident waves from higher chamber pressures since the ratio of incident to reflected pressures increases with pressure while the ratio of incident shock pressure to chamber pressure decreases.

The excess pressure in the reflected wave, P_r , is related to the excess pressure in the incident wave, P_i , by

$$P_r = 2P_i \left[\frac{7P_o + 4P_i}{7P_o + P_i} \right],$$

where P_o is the absolute pressure ahead of the incident shock. In the experiments reported here P_o was atmospheric pressure.

The pressure P_r will act at the closed end of the expansion chamber until (i) the arrival of the rarefaction reflected from the closed end of the compression chamber or (ii) the arrival of a secondary reflection from the variable-density region at the boundary separating the gas that was originally in the compression chamber from the gas that was originally in the expansion chamber.

The time t between the arrival of the incident shock at the closed end of the expansion chamber of length L_e and the arrival of the reflection from the gas boundary is given by

$$t = \frac{L_e}{a_o} \left(\frac{y + 6}{y} \right) \left(1 + \sqrt{\frac{2y + 5}{8y - 1}} \sqrt{\frac{1}{7(1 + 6y)}} \right),$$

where y is the incident shock strength (that is, ratio of absolute pressures ahead of and behind the incident shock) and a_o is the velocity of sound in the medium ahead of the incident shock. This time t will be the interval

during which the pressure at the end of the tube will be P_r provided that the ratio of the length of the compression chamber, L_c , to the length of the expansion chamber, L_e , is equal to or above a certain minimum given by

$$\frac{L_c}{L_e} = \left(\frac{1}{2\sqrt{7(1+6y)} + 4(y-1)} \right) \left(\frac{8y+6}{y} \right) \left(1 - \frac{y-1}{\sqrt{7(1+6y)}} \right),$$

which is necessary to delay the arrival of the rarefaction wave from the closed end of the compression chamber.

These formulas were derived from the simple theory of the formation of the shock wave, but experiment has proved them quite adequate for design purposes.

2. Tube theory

The simple theory of shock-wave formation given in Sec. 3 of Reynolds' report^{1/} is inadequate for several reasons, the chief of which are the following.

- (1) The wave is not initially plane since the cellophane is bulged out at the time it shatters (Fig. 7). In proceeding down the tube the wave becomes plane as the components of velocity normal to the axis of the tube are cancelled by multiple reflections from the walls of the tube. Thus the problem is originally three-dimensional and becomes one-dimensional only after the wave has progressed a certain distance down the tube. However, the simple theory treats the problem entirely from a one-dimensional standpoint and consequently represents only an approximation.
- (2) The compression wave traveling into the expansion chamber is not initially a shock because the diaphragm does not shatter instantaneously. However, this compression wave will become a shock after proceeding a certain distance down the expansion chamber. Photographs indicate that the wave has become a plane discontinuity after progressing less than 3 ft from the diaphragm. The final pressure in the step shock will depend on the process by which the adiabatic wave becomes a discontinuity. However, in the simple theory no analysis is made of this process.

The closeness of the approximation will be a measure of the degree to which the actual process of formation of the shock wave approaches the simple idealization.

The most direct method of determining shock pressures consists of measuring the shock-front velocity V and computing the excess shock pressure P from the pressure-velocity equation

$$P = \frac{2\gamma P_0}{\gamma + 1} \left[\frac{V^2}{a_0^2} - 1 \right],$$

in which P_0 is the pressure ahead of the shock, γ is the ratio of specific heats, and a_0 the velocity of sound in the medium ahead of the shock.

Three questions arise concerning the accuracy of pressures determined in this way.

(i) The validity of the pressure-velocity equation. This equation is derived from the Rankine-Hugoniot relations and the ideal gas law. The Rankine-Hugoniot relations are the laws of conservation of mass, momentum, and energy applied to shock waves and are generally accepted without question. However, since the experiments are done in air, which is not an ideal gas, the assumption of the ideal gas law is to some extent questionable. A second approximation to the real pressure-velocity relation may be obtained by using van der Waals equation in the derivation instead of the ideal gas law. This will give the first-order correction term in the pressure-velocity relation for a real gas.

The derivation of the pressure-velocity relation using van der Waals equation has already been reported^{9/}. The result of the derivation was that the assumption of a "van der Waals" gas rather than an ideal gas would change the computed pressures by an amount within the experimental error of blast-tube work.

(ii) The determination of a_0 . The velocity of sound ahead of the shock, a_0 , is determined from the formula

$$a_0 = \sqrt{\frac{\gamma P_0}{\rho_0}},$$

^{9/} "Pressure-velocity relations for shock waves in a van der Waals gas," by W. T. Read, included in AES-9 (OSRD-5011).

where P_o , ρ_o , and γ_o are the pressure, density, and ratio of specific heats, respectively, in the medium ahead of the shock.

The medium ahead of the shock in the blast tube is a mixture of air and water vapor. Letting the subscript a refer to air, the subscript w to water vapor, and the subscript o to the mixture we have:

$$P_o = P_a + P_w = P_a \left[1 + \frac{P_w}{P_a} \right],$$

$$\rho_o = \rho_a + \rho_w = \rho_a \left[1 + \frac{\rho_w}{\rho_a} \right].$$

To determine γ_o we use the relations $\rho_o C_{v_o} = \rho_a C_{v_a} + \rho_w C_{v_w}$ and $C_v = R/M(\gamma - 1)$, where the C_v 's are specific heats per unit mass at constant volume, R is the gas constant, and M is the molecular weight.

Substituting for the C_v 's and dividing by R we obtain:

$$\frac{\rho_o}{M_o(\gamma_o - 1)} = \frac{\rho_a}{M_a(\gamma_a - 1)} + \frac{\rho_w}{M_w(\gamma_w - 1)}.$$

Using the ideal gas law $P\rho = RT/M$ we have for γ_o

$$\gamma_o = \gamma_a \frac{\left[1 + \frac{\gamma_w (\gamma_a - 1) P_w}{\gamma_a (\gamma_w - 1) P_a} \right]}{\left[1 + \left(\frac{\gamma_a - 1}{\gamma_w - 1} \right) \frac{P_w}{P_a} \right]}.$$

Since P_w is small in comparison with P_a we will drop second and higher-order terms in P_w/P_a . This gives for a_o

$$a_o = \sqrt{\frac{\gamma_a P_a}{\rho_a}} \left[1 + \frac{1}{2} \left\{ 1 - \frac{M_w}{M_a} + \frac{\gamma_a - 1}{\gamma_w - 1} \left(\frac{\gamma_w}{\gamma_a} - 1 \right) \right\} \frac{P_w}{P_a} \right].$$

Substituting the numerical values for the γ 's and M 's for air and water gives

$$a_o = \sqrt{\frac{\gamma_a P_a}{\rho_a}} \left[1 + 0.149 \frac{P_w}{P_a} \right].$$

If a_s is the velocity of sound in air at $0^\circ C$ and for zero humidity we derive

$$a_o = a_s \sqrt{1 + \frac{t_o}{273}} \left[1 + 0.149 \frac{P_w}{P_a} \right],$$

where t_o ($^{\circ}\text{C}$) is the temperature of the air ahead of the wave in the blast tube. In the velocity experiments t_o was around normal room temperature.

This derivation has assumed an ideal gas. However, the final result would be unchanged if van der Waals correction terms were introduced since the corrections in a_o and a_s would be approximately equal and would cancel for values of t_o around normal room temperature.

(iii) The accuracy of the velocity measurement. This will be discussed in Part II.

It has become customary to speak of excess shock-wave pressure \underline{P} as a function only of excess compression-chamber pressure P_c . Actually P_o is involved in the relation, \underline{P}/P_o being a function of P_c/P_o . The variation of \underline{P} with P_o for constant P_c may be derived as follows:

$$\frac{\underline{P}}{P_o} = f\left(\frac{P_c}{P_o}\right), \quad \frac{\partial \underline{P}}{\partial P_c} = f',$$

$$\frac{\partial \underline{P}}{\partial P_o} = f - \frac{P_c}{P_o} f' = \frac{\underline{P}}{P_o} \left[1 - \frac{P_c}{\underline{P}} \frac{\partial \underline{P}}{\partial P_c} \right],$$

$$\frac{\partial \log \underline{P}}{\partial \log P_o} = 1 - \frac{\partial \log \underline{P}}{\partial \log P_c}.$$

Since $\partial \log \underline{P} / \partial \log P_c$ is near to unity the percentage change in \underline{P} will be a small fraction of the percentage change in P_o . In gauge calibration P_o is atmospheric pressure and will vary by very small percentages. Therefore, the change in \underline{P} due to normal changes in P_o will be negligible and \underline{P} may justifiably be regarded as a function only of P_c .

II. TECHNIQUE AND RESULTS OF VELOCITY MEASUREMENTS

1. Velocity techniques

The system of measuring shock velocity by means of schlieren pulses has been previously described.^{10/} However, because of some changes that have been made in the technique in applying it to this particular shock tube, it seems advisable to outline the procedure involved. In Figs. 12 and 13 A is a section of the tube having the same inside configuration as the rest of the expansion chamber. Four ports, a, b, c, and d, are arranged in pairs at right angles to the tube separated by 31 in. Flat glass windows $\frac{1}{4}$ in. in diameter are fitted into the ports in such a way as to cause as small a disturbance as possible in the flow of the air inside the tube. Light from a vertical, coiled filament is collimated in a narrow beam $\frac{3}{8}$ in. high and about 0.05 in. wide by two vertical slits, passes across the shock tube through small glass windows and falls on a photocell (type 931). A vertical knife-edge on the opposite side of the tube from the light source cuts off most of the light beam. As the shock front crosses it, the beam is refracted slightly and the light on the photocell momentarily increases. Thus an electrical pulse is produced whose total duration has been found by a single-sweep oscillograph and wide-band amplifier to be about 1.5 μ sec (Fig. 14). The pulse from the first light screen met by the shock is made to start the chronograph while that from the second screen turns it off. The velocity of the shock is, of course, the ratio of the distance between knife-edges to the time measured by the chronograph."^{10/}

These photocells are followed by a preamplifier E (Fig. 12) and a wide-band amplifier to amplify the pulse sufficiently to operate the chronograph.^{11/} Because of the distortion in time intervals in this instrument a blanking

^{10/} Photographic investigation of the reflection of plane shocks in air, by L. G. Smith, NDRC Report A-350 (OSRD-6271).

^{11/} A complete description of this chronograph will be found in Short base line projectile velocity measurements, by R. J. Emrich and L. A. Delsasso, NDRC Report A-89 (OSRD-927).

signal is applied to the control grid of the cathode-ray tube to give a timing signal every $5 \mu\text{sec}^{12/}$

Several factors in this procedure may lead to incorrect results and it may be well to mention them here. First, the light screens must be vertical (or parallel to the shock front), the two lights must give parallel beams, and the knife-edges must be parallel. It is also necessary to measure accurately the distance between the knife-edges. It seems also advisable to cut off equal amounts of the beam before it strikes the photocell. Inasmuch as the noise level of the photocells and amplifiers is considerable, it is desirable to get as well-defined a beam as possible with practically no scattering.

Mounting the lights and knife-edges apart from the tube eliminates heating of the tube and, with the knife-edges mounted thus, they are not affected by the recoil. It is necessary, however, to have the tube secure, so that the narrow windows will not move out of line when the tube is fired. It is also desirable to photograph the chronograph pattern to facilitate easy reading of the time interval. This can be done satisfactorily with Super XX at f:6, exposing the film for just the initial flash of the cathode-ray tube. The over-all accuracy obtained by such a system is certainly within 0.1 percent of the true velocity.

In the computation of the strength of a shock from its velocity it is necessary to know the velocity of sound in air, correction being necessary for both temperature and relative humidity. A calibrated thermometer and thermocouples were placed inside the tube and removed just before the diaphragm was broken. Wet- and dry-bulb thermometer recordings determined the relative humidity. An accurate measure of the pressure in the compression chamber was necessary and this was made by means of a multiple manometer, which will be discussed later.

2. Discussion of velocity results

With the apparatus that has been described, about 200 shots were taken under various conditions and at irregular intervals over a period from June 26, 1945, until Aug. 21, 1945.

^{12/} "Projectile velocity measurements with light screens and spiral chronograph," by R. J. Emrich and L. I. Shipman, included in OTB-9 (OSRD-4948).

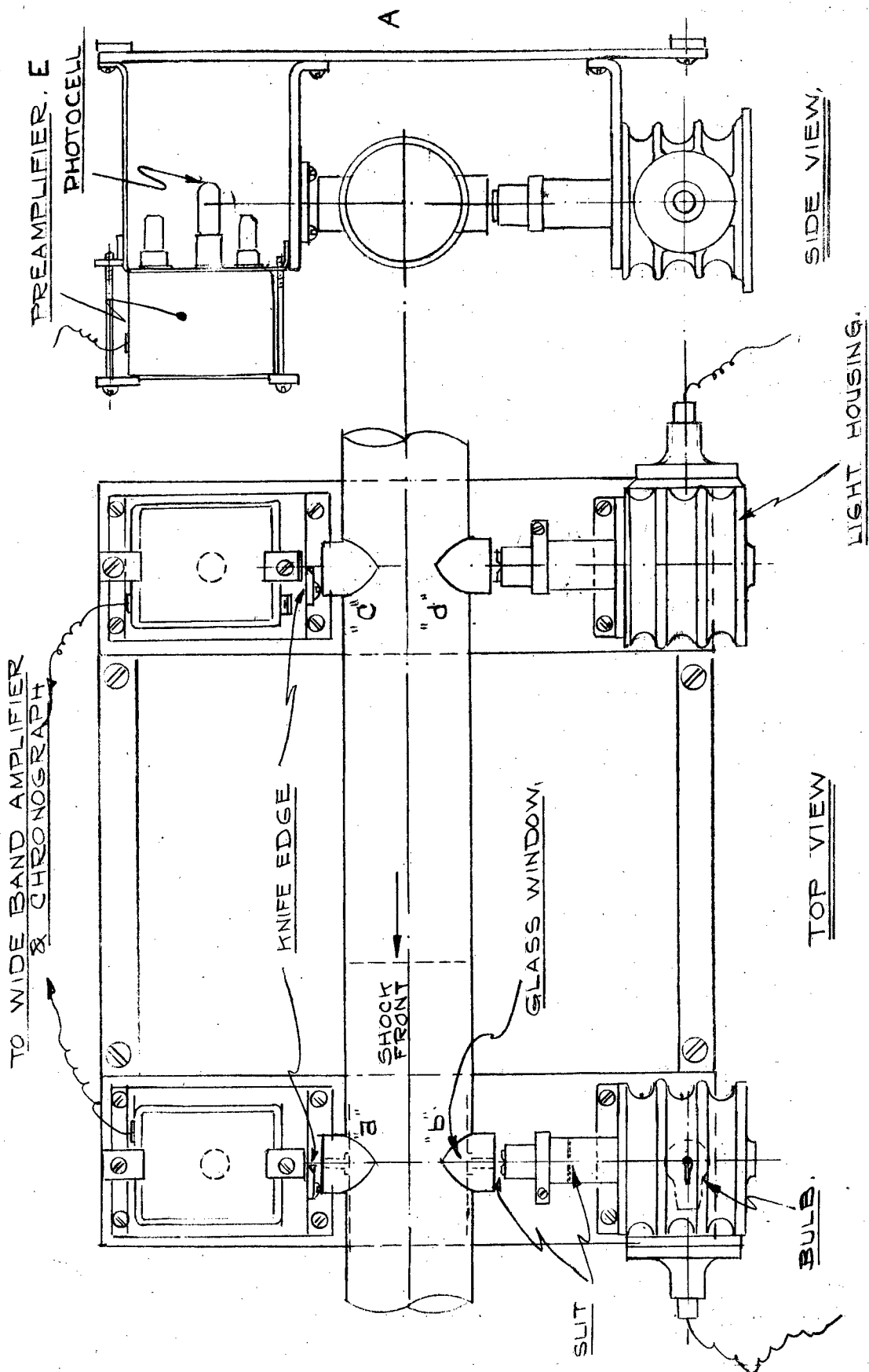


Fig. 12. Velocity section.

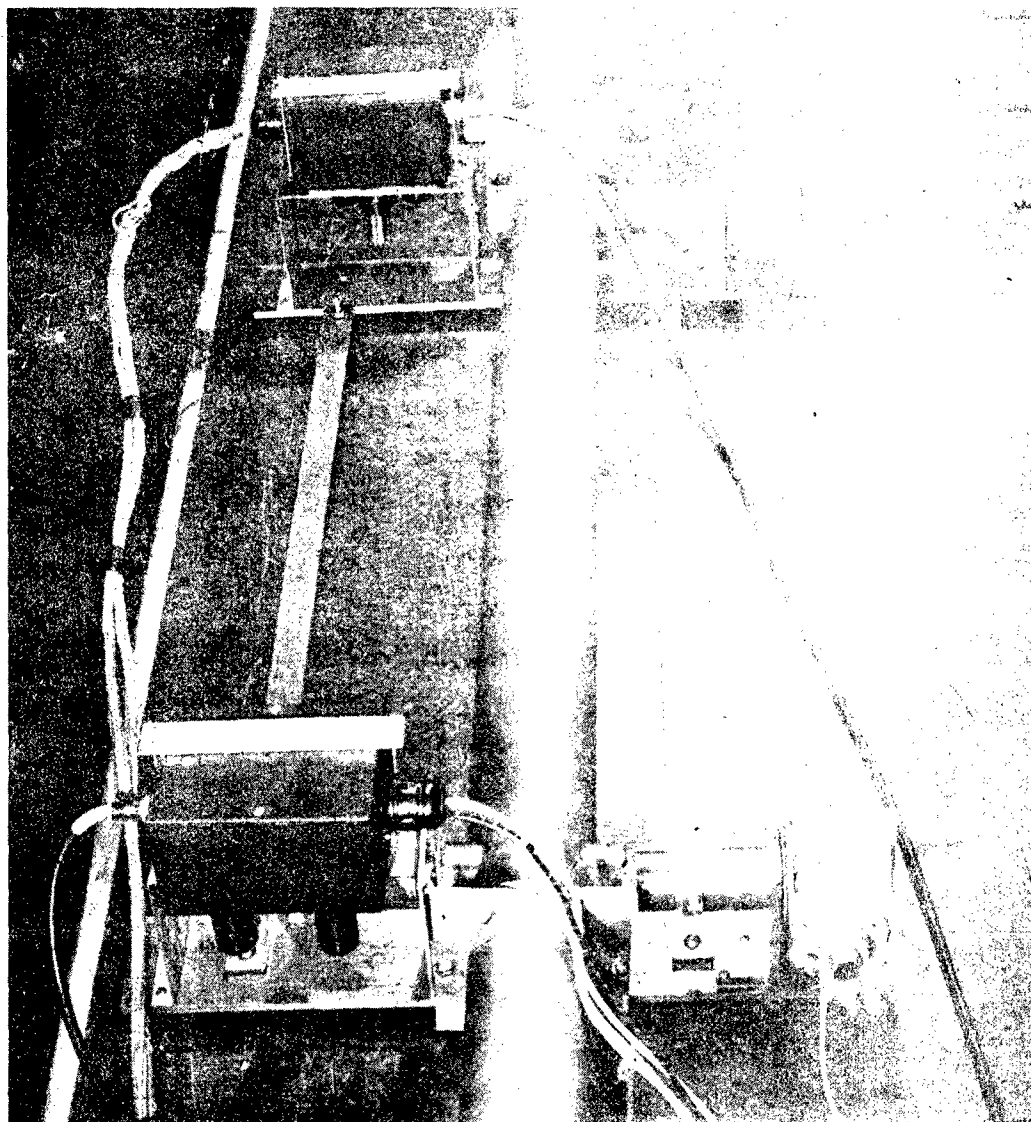


Fig. 13. Velocity unit in place.

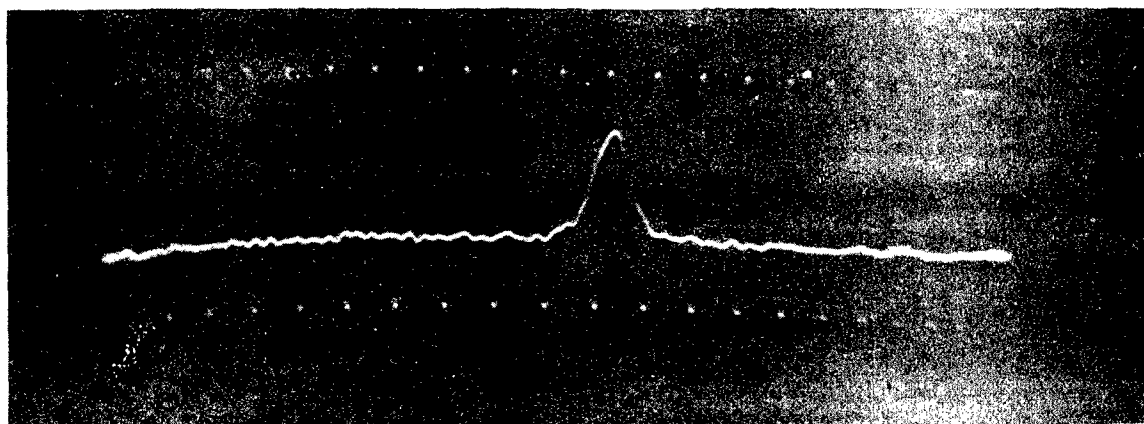


Fig. 14. Schlieren pulse of shock passing light screen (timing trace of 1 megacycle/sec).

In tabulating results it has been found convenient to express shock-wave pressures, computed from velocities, in terms of their percentage deviations from the theoretical pressures given by the simple idealized theory of shock formation discussed in Part I. It should again be mentioned that the theoretical pressures are only approximations and are not expected to agree with pressures computed from accurate velocity measurements.

Recording shock pressures in terms of their percentage deviations from the corresponding theoretical pressures makes it possible to present results in a simple nondimensional form and, at the same time, to indicate the degree to which actual shock formation approximates the idealized picture.

In all cases pressures determined from velocities are lower than the theoretical pressures. The recorded values of percentage deviation represent percentages below theory and are, therefore, always positive.

(a) First set of shots. -- The first set of shots was made using alternately either a 9-ft or 3-ft expansion chamber preceding the velocity section (about $10\frac{1}{2}$ ft and $4\frac{1}{2}$ ft, respectively, to the center of the velocity baseline from the diaphragm). The shots were made over a compression-chamber pressure range of 7 to 73 lb/in² and were done in a more or less random order, which would give an indication of the scatter over a period of time. Curves 1 and 2 of Fig. 15 are plots of the data taken at $10\frac{1}{2}$ ft and $4\frac{1}{2}$ ft, respectively, from the diaphragm, showing the percentage difference ($100 \Delta P/P_{th}$) below the theoretical pressures computed from simple theory, as a function of compression chamber pressure P_c . The standard error for every set of shots is shown and is seen to be of the order of 1 percent. Smooth curves are drawn through each of the two groups of data and root-mean-square deviations were computed for each of the curves, giving 1.4 percent for Curve 1 and 0.9 percent for Curve 2. From these smooth curves, Table I was prepared. The first column gives the chamber pressure P_c (lb/in²); the second, the theoretical shock-wave pressure P_{th} ; the third, the measured shock-wave pressure at $10\frac{1}{2}$ ft, P_{10} ; and the last, at $4\frac{1}{2}$ ft, P_4 . A plot of these last three columns as a function of the first, appears in Fig. 16. It is quite evident that the differences in pressure between the two lengths diminish as the pressure increases, the difference being 6 percent at the low end and $3\frac{1}{2}$ percent at the high end.

A comparison of these results with the calibration of L. G. Smith's rectangular tube^{10/} is of interest.

In the rectangular tube large pressure ratios were obtained for relatively low pressure differences by evacuating the expansion chamber. By this technique pressure ratios were obtained that would have required 2200 lb/in² in the compression chamber had the expansion chamber been left at atmospheric pressure. The velocities were measured at a distance of 6 ft from the diaphragm. The value of sound velocity a_0 used by Smith was approximately 0.5 percent low due to neglect of humidity and use of an incorrect value for the velocity of sound at 0°C. Table II gives Smith's results scaled to an expansion-chamber pressure of 14.7 lb/in² and corrected for the velocity of sound. In making the correction, a humidity of 60 percent, considered reasonable since the experiments were performed in summer, was assumed. The third column in Table II gives the deviation of Smith's results from theory. As in all references to deviations from theory, it is understood that the deviations are measured in the negative direction; that is, experimental pressures are always lower than theoretical.

Between compression-chamber pressures of 7 and 40 lb/in² the results on the rectangular tube are within 3 percent of the results obtained at 4½ ft in the present tube. Above 40 lb/in² in the compression chamber, the discrepancy between the tubes is somewhat greater and at 70 lb/in² is around 6 percent, the rectangular tube giving results nearer to the theoretical, that is, higher.

Smith's results were obtained without the use of a blanking signal on the chronograph. It is now known that this omission could cause as much as 0.3 percent error in the chronograph reading. This error, in turn, could cause errors in pressure from 4 percent at 7 lb/in² to 1 percent at 70 lb/in² in the compression chamber.

Comparison of the present data with the results of two previous programs of velocity measurements in gauge calibration tubes is also of value.

In September 1944^{2,3/} shock-front velocities were measured at 4½ ft from the diaphragm in a tube of the same internal cross section as the present tube but of the older design and construction. The velocity-measurement setup was the same as the present one except that narrow cellophane-covered slits were used instead of glass windows in the velocity section. Also, no

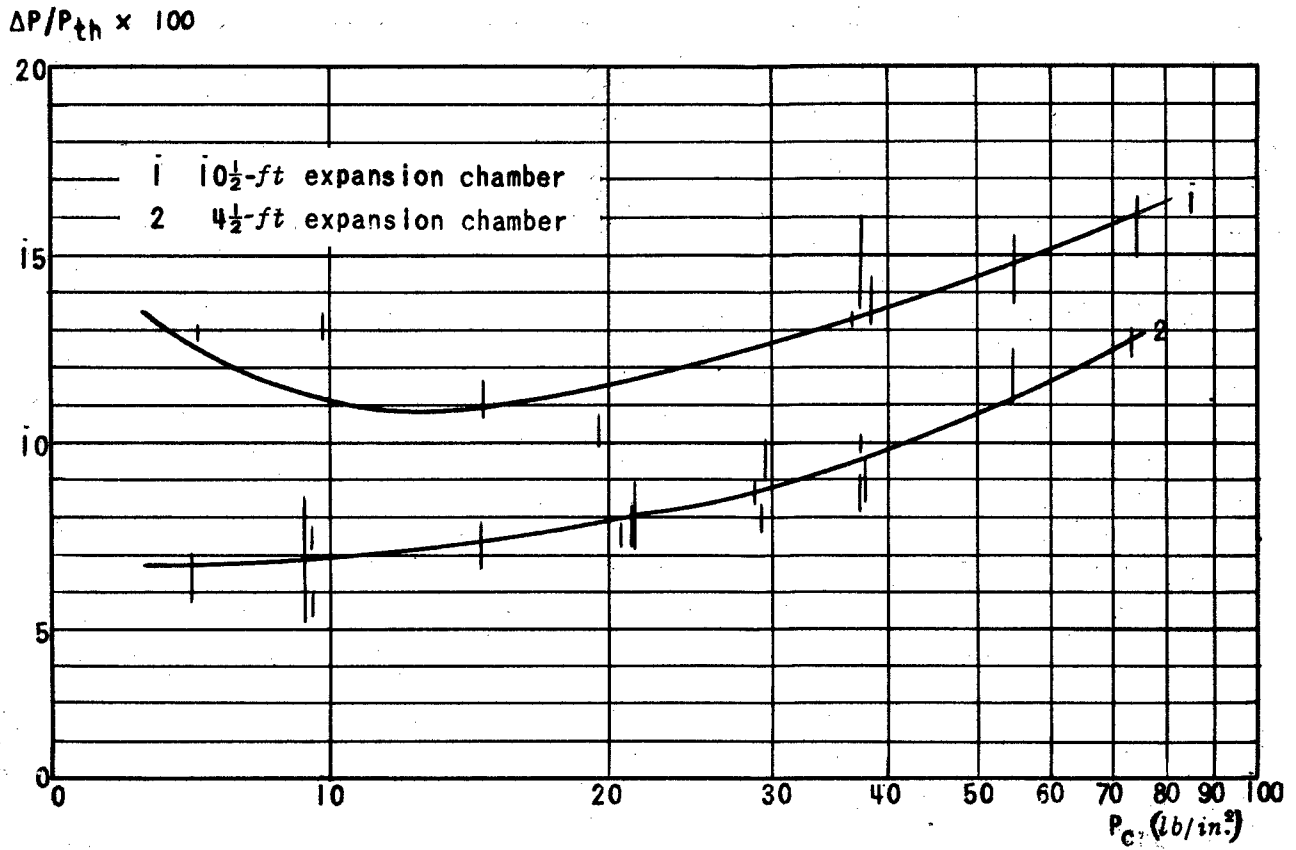


Fig. 15. Percentage deviation from theoretical shock-wave pressure vs chamber pressure.

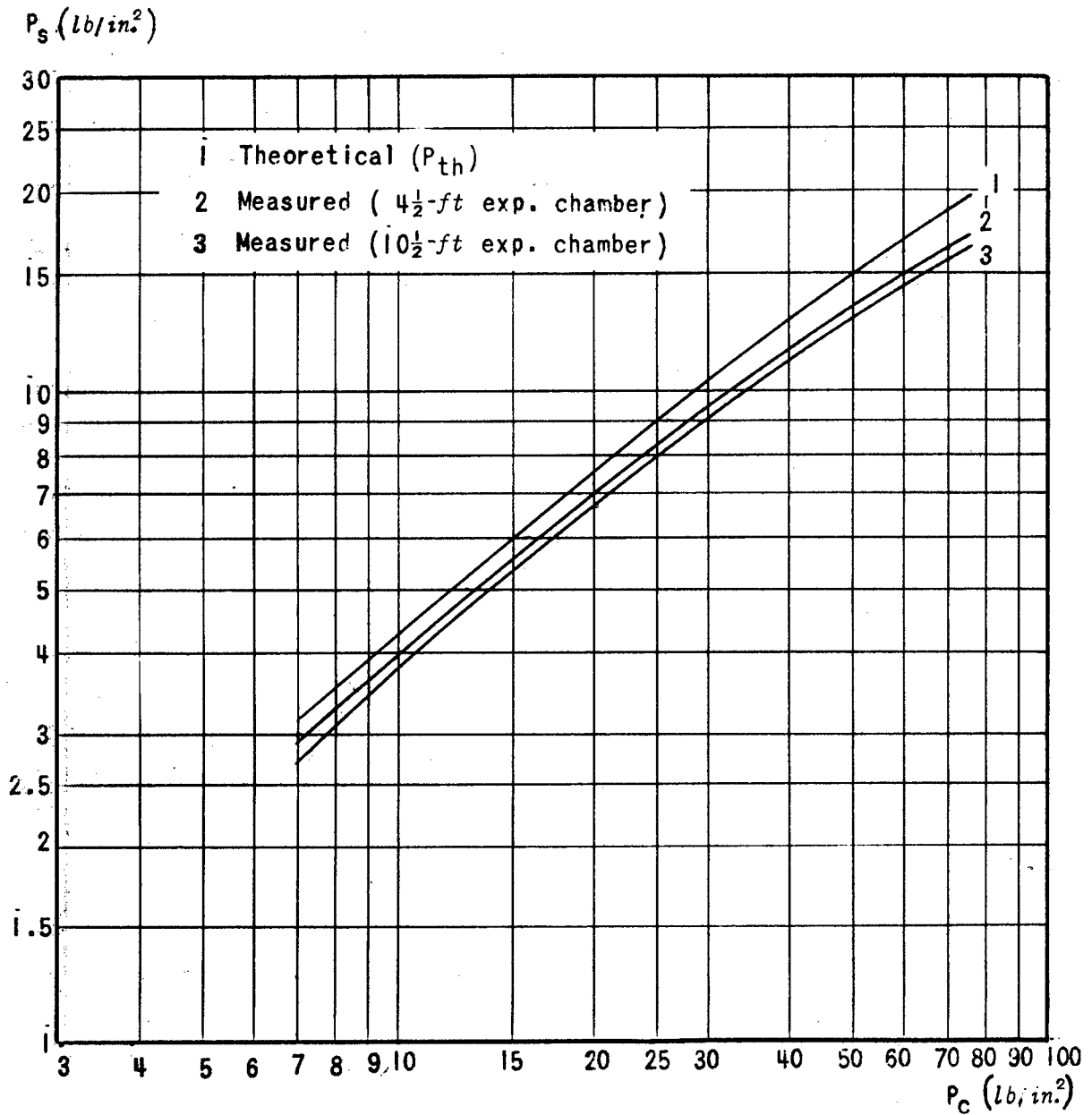


Fig. 16. Shock-wave pressure vs compression-chamber pressure in blast tube.

Table I. Theoretical and measured shock-wave pressures versus chamber pressure.

P_c (lb/in ²)	P_{th} (lb/in ²)	P_{10}^* (lb/in ²)	$P_{1/2}^{**}$ (lb/in ²)
7	3.115	2.719	2.905
8	3.510	3.089	3.271
9	3.885	3.439	3.614
10	4.260	3.783	3.964
11	4.620	4.112	4.294
12	4.980	4.440	4.626
13	5.325	4.750	4.942
14	5.670	5.056	5.257
15	6.010	5.351	5.565
16	6.335	5.632	5.857
18	6.975	6.187	6.435
20	7.575	6.704	6.990
22	8.17	7.21	7.52
24	8.74	7.69	8.02
26	9.30	8.16	8.51
28	9.83	8.60	8.98
30	10.34	9.03	9.42
32	10.86	9.465	9.88
36	11.82	10.26	10.71
40	12.73	11.00	11.49
44	13.67	11.73	12.25
48	14.47	12.41	12.94
52	15.27	13.04	13.62
60	16.81	14.25	14.93
68	18.25	15.37	16.01
76	19.58	16.41	17.04

* Shock-wave pressure at 10 $\frac{1}{2}$ ft.

** Shock-wave pressure at 4 $\frac{1}{2}$ ft.

Table II. Results in rectangular tube with evacuated expansion chamber.
Pressures scaled to an expansion-chamber pressure of 14.7 lb/in²

P_c (lb/in ²)	P_{shock}	
	(lb/in ²)	Percentage Below Theoretical Value
5.98	2.38	18.85
8.75	3.46	8.95
12.22	4.67	7.52
16.64	6.06	7.48
29.85	9.52	7.48
39.64	11.73	7.42
53.04	14.37	7.29
71.77	17.60	6.68
100.14	21.64	6.40

blanking signal was used and the humidity was not measured. The results, which were quite consistent over the range of pressures used (10 to 14 lb/in² in the compression chamber), gave shock pressures around 4 percent below the theoretical values. The correction for humidity would make the shock pressures approximately 7 percent lower than theory. This agrees well with present results.

In the September 1944 tests, shots were taken to determine decay of the shock pressure for a chamber pressure of 10 lb/in². The results showed only 0.6 percent decay between 4 $\frac{1}{2}$ ft and 7 $\frac{1}{2}$ ft from the diaphragm. This is less than would be predicted from present data which show 4 percent decay between 4 $\frac{1}{2}$ ft and 10 $\frac{1}{2}$ ft from the diaphragm at a chamber pressure of 10 lb/in².

In December 1944^{3/} velocities were measured using the same expansion chamber and velocity section used in September with the present compression chamber. Humidity was measured but no blanking signal was used. Table III gives the percentage deviation from theory for the December results together with the corresponding deviations for the present data. The agreement at the four lower pressures is quite encouraging. At the two higher pressures the December measurements of chamber pressure were made with an Ashton gauge of the Bourdon type, which is less accurate than a manometer. This may account in part for the discrepancies (maximum of 3.3 percent) at the higher pressures. In summarizing the comparison of different calibrations at different times and for different tubes the following conclusions may be drawn:

- (1) For compression-chamber pressures of 7 to 40 lb/in² and at 4 $\frac{1}{2}$ to 6 ft from the diaphragm all of the results on all of the tubes used, including the rectangular tube, agree within 3.3 percent if the earlier results are corrected for humidity. Of the several calibrations the most recent is regarded as the most reliable. The earlier results are less certain because of the absence of a blanking signal on the chronograph.
- (2) For compression-chamber pressures from 40 lb/in² to 70 lb/in² the most recent and only results are a maximum of 6 percent below (further from theory than) results obtained at the same pressure ratios using a rectangular tube with the expansion chamber evacuated. It is not known whether this difference is due to the difference in shape of the tubes, to the difference

in initial expansion chamber pressure, or to some experimental error.

- (3) Recent results indicate a decay of shock-wave pressure of 3 to 6 percent between $4\frac{1}{2}$ ft and $10\frac{1}{2}$ ft from the diaphragm. The reason for the decay is not known. Some earlier results based on fewer shots show a smaller rate of decay and suggest that the decay may depend on the tube.

Table III. Previous velocity measurements* compared with present data.

P_c (lb/in ²)	P_{th} (lb/in ²)	$100\Delta P/P_{th}$	
		Previous Data	Present Data
7.62	3.11	7.5	6.8
10.02	3.99	6.5	6.95
12.38	4.80	6.1	7.2
14.62	5.53	5.9	7.35
25.5	8.55	6.2	8.5
35.5	10.99	6.1	9.35

* Taken from Table I of "Determination of shock-wave pressure in the blast tube as a function of compression-chamber pressure," by W. T. Read, included in AES-5 (OSRD-4514).

It is suggested that anyone constructing a blast tube (and not desiring to measure velocities) calibrate gauges at $4\frac{1}{2}$ ft from the diaphragm, where the pressure is fairly well known and apparently independent of the tube, and then use the calibrated gauges to investigate the distribution of pressure farther down the expansion chamber.

(b) Shots made to determine effect of varying number of sheets of cellophane. -- Two groups of shots were made to determine the effect of varying the number of sheets of cellophane used. The first 9 shots were made with a pressure of 10 lb/in² in the compression chamber using 1, 2, and 3 pieces of cellophane (3 shots each) and the next 8 were at 15 lb/in² using also 1, 2, and 3 pieces (the breaking point of one piece was known to be at about 20 lb/in²). In none of these cases was the deviation in shock pressure observed greater than 0.8 percent.

Note that the September tests^{2/} showed that when a large handful of small pieces of cellophane was scattered throughout the tube the shock-wave pressure decreased by 1.5 percent. From these experiments it was concluded that bits of shattered cellophane should be cleared from the tube frequently, but not necessarily after every shot since the amount of cellophane accumulating from a single shot is extremely small.

The September tests also showed that when the 3-ft section ahead of the velocity section was turned through 60°, thus introducing a pronounced irregularity in the cross section of the tube, the shock pressure decreased by 3 percent. Since so large an irregularity caused only a 3-percent discrepancy, it was concluded that minor local irregularities would have a negligible effect. However, it should not be concluded that a continuous curvature in a long tube would have no effect; until this question has been fully investigated it is felt that care should be taken to make the tube straight.

The December tests showed that shock-wave pressure is independent of temperature. It has also been shown theoretically that variations in the carbon dioxide content of the air, small differences in temperature between compression chamber and expansion chamber (less than 5 deg C) and deviations of the air from an ideal gas, introduce errors all less than 1 percent.

(c) Effort to measure velocity of shock reflected from closed end of tube. — For the next set of experiments the knife-edges were reversed and an effort was made to measure the velocity of a shock reflected from the closed end of the tube. The expansion chamber used was 14 ft long, the compression chamber 5 ft, and the center of the velocity baseline was 10½ ft from the diaphragm. These dimensions were chosen so that the reflected shock front had passed the second knife-edge some time before either the temperature discontinuity or the rarefaction from the compression chamber reached the knife-edge.

The excess pressure behind the reflected wave, P_r , is related to the reflected shock-front velocity, V_r , by

$$6 \left(\frac{P_r + P_o}{P_i + P_o} \right) = 7 \left(\frac{V_r + u_i}{a_i} \right)^2 - 1,$$

where u_i and a_i are, respectively, the particle velocity and the velocity of

sound behind the incident shock, P_i is the excess incident pressure, and P_o is the absolute pressure ahead of the incident shock. In these experiments P_o was atmospheric pressure. Since u_i and a_i are given by

$$\left(\frac{u_i}{a_o}\right)^2 = \frac{25}{7} \frac{P_i^2}{P_o(7P_o + 6P_i)},$$

$$\left(\frac{a_i}{a_o}\right)^2 = \left[\frac{P_i + P_o}{P_o}\right] \left[\frac{7P_o + P_i}{7P_o + 6P_i}\right],$$

where a_o is the velocity of sound ahead of the incident shock, we have for P_r as a function of V_r , P_i , a_o , and P_o

$$P_r = \frac{1}{6(P_i + 7P_o)} \left[\frac{V_r}{a_o} \sqrt{7P_o(6P_i + 7P_o)} + 5P_i \right] - \left[\frac{7P_o + P_i}{6} \right].$$

The incident pressures were determined from Table I; P_o and a_o were determined as in the previous experiments; and V_r was measured as described in the foregoing. The values of P_r obtained in this way from 12 shots at 3 different pressures are recorded in Table IV as $P_{r(\text{meas})}$.

The foregoing formulas depend only on the Rankine-Hugoniot relations and the ideal gas law. If, however, we add the condition that the particle velocity at the reflecting wall must be zero, then it is possible to derive the following relation which does not depend on V_r :

$$P_r = 2P_i \left(\frac{7P_o + 4P_i}{7P_o + P_i} \right).$$

Table IV. Velocity measurement of reflected shock-wave pressures.

P_c (lb/in ²)	P_i (lb/in ²)	$P_{r(\text{th})}$ (lb/in ²)	$P_{r(\text{meas})}$ (lb/in ²)	$P_{r(\text{th})} - P_{r(\text{meas})}$ (percent)
9.33	3.57	7.85	7.48 ± 0.02	4.7
14.7	5.24	12.0	11.39 ± 0.03	5.1
19.1	6.49	15.25	14.29 ± 0.07	6.3

Values of P_r determined from the P_i 's in Table I by this formula are recorded in Table IV as $P_{r(th)}$, and are around $5\frac{1}{2}$ percent above the corresponding values of $P_{r(meas)}$. It is well to point out here that these results are tentative and it is regretted that because of limited time more work was not done to determine this difference (if it is a real difference) over a wide range of pressures, expansion chamber lengths, reflecting walls, and so forth.

III. PIEZOELECTRIC GAUGES, ELECTRONIC APPARATUS, AND OTHER EQUIPMENT

1. Characteristics of flush and wafer quartz gauges

(a) "English" gauges. -- The first quartz pressure gauges used at the Princeton Station were similar in design to the gauges developed in England, particularly at the Road Research Laboratory. They consisted of a heavy steel case with a cylindrical well in which the crystals were set, covered by a closely fitting steel plunger. These gauges have been described in more detail in previous reports.^{13/} Their chief fault was air leakage around the plunger, which required careful sealing of the face of the gauge with grease, rubber diaphragms, or other means, since the edges of the quartz crystals must be protected from pressure in order to obtain any response.

(b) The Smith gauge. -- The second general type of quartz gauge constructed at the Princeton Station was designed by L. G. Smith, to provide a permanent sealing of the interior of the gauge from external pressure. This was accomplished by adding a flange to the sensitive face plate of the gauge and placing a rubber gasket between the flange and the gauge body. Several designs were developed, involving minor differences in such matters as the number and arrangement of the gaskets. A typical design is shown in Figs. 17, 18, and 19.

The response of these gauges to shock waves was found to be subject to vibrations of considerable magnitude, with a frequency of the order of 10 to 20 kc/sec, unless the gauges were carefully made and adjusted in assembly. The contact between the crystal and the electrodes is maintained in these gauges by the net pressure exerted by the compressed rubber gaskets and was found to be quite critical. The easiest way of adjusting this pressure was found in practice to be the addition of layers of lead foil, from 0.001 to 0.005 in. thick, between the elements of the crystal pile until a minimum of vibrations or "hash" was observed. Gauges of this design, constructed with brass cases, were called type "S." A few gauges of the same design, but with steel cases, were called type "T."

^{13/} The measurement of transient stress, displacement, and pressure, by C. W. Lampson, NDRC Report A-73 (OSRD-756); Small charge air blast experiments, by G. T. Reynolds, NDRC Report A-191 (OSRD-1518); and A.R.D. Explosives Report 48/44.

A variation of the design, labeled type "R," is shown in Fig. 20. The plug which screws in from the back allows easier adjustment of the pressure holding the crystal pile together, but also makes the gauge more subject to changes in behavior, due to possible loosening of the plug under field conditions. An improvement is the incorporation of set screws to hold the plug in position, which can be done without difficulty.

Quartz gauges of these types were used in several field programs at the Princeton Station Proving Ground (notably the ground reflection and Mach reflection investigations^{14/}) and in shock-tube measurements. Over a period of months they were found to be subject to apparently erratic changes in sensitivity when calibrated in the shock tube, the cause of which was not determined until W. T. Read observed that the sensitivities of both quartz and tourmaline gauges varied with temperature in some cases as described in AES-10^{15/}

Further investigation of this phenomenon in the type "R" and type "S" quartz gauges showed that the temperature dependence was not a direct function of temperature but that heating or cooling produced permanent changes in the properties of the gauge. (In this respect the effect is different from that observed in tourmaline gauges.) Figure 21 shows the behavior of a gauge during a typical sequence of tests. It was observed that tightening or loosening the gauge (increasing or decreasing the static pressure on the crystal pile) produced changes in sensitivity similar to those produced by temperature changes. Hence it is now believed that the temperature effect is in fact a static pressure effect, due to changes in the static pressure on the crystal pile produced by differential expansion of the case and the components of the pile, combined with a packing of the lead-foil layers or of the rubber diaphragms, which makes the changes irreversible. Since a search of the literature has indicated that the piezoelectric constant for

^{14/} "Peak pressure dependence on height of detonation," by A. H. Taub, included in AES-1 (OSRD-4076).

"Impulse dependence on height of detonation," by R. G. Stoner and A. H. Taub, included in AES-2 (OSRD-4147).

"Mach reflection of shock waves from charges detonated in air," by R. G. Stoner, included in AES-3 (OSRD-4257).

^{15/} "Effect of temperature on gauge calibration," by W. T. Read, included in AES-10 (OSRD-5144).

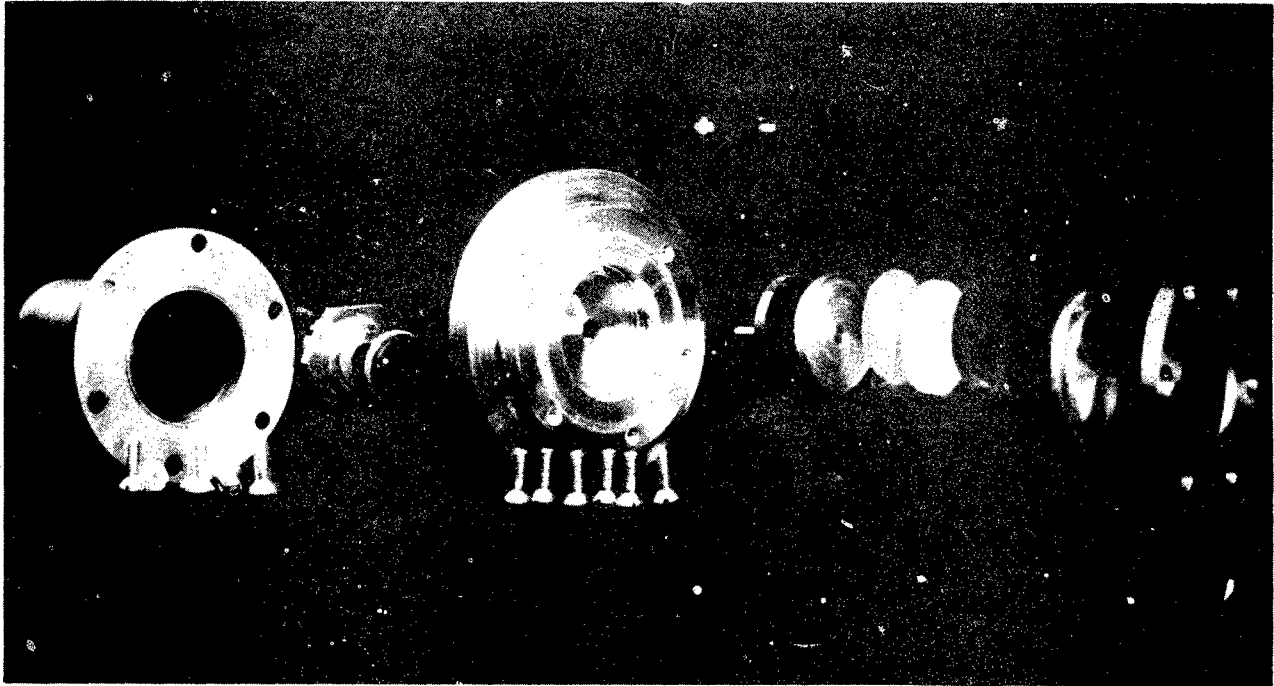


Fig. 17. Type "S" gauge assembly with waterproof cable housing.

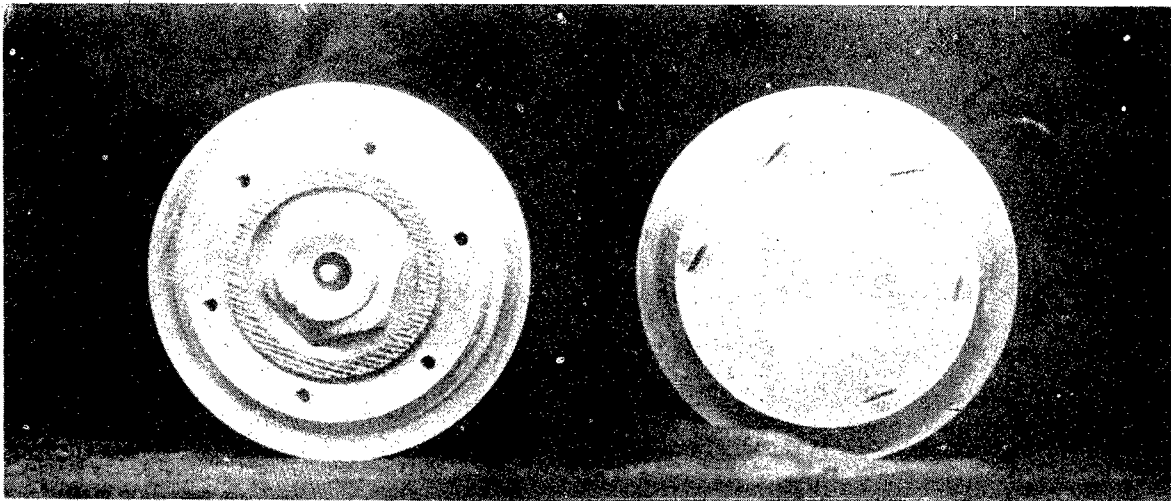


Fig. 18. Assembled type "S" gauge.

- A. Quartz crystal
- B. Rubber gasket
- C. Gasket grooves
- D. Center electrode
- E. Gauge block
- F. Bakelite insulator
- G. Sensitive face

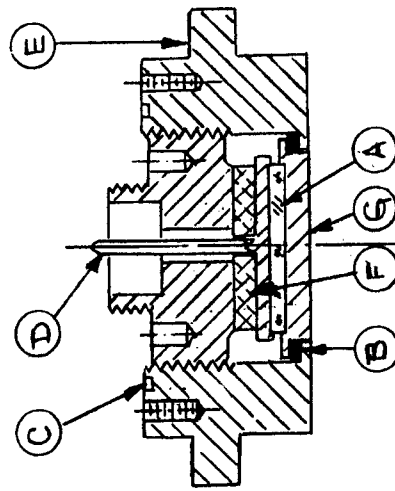
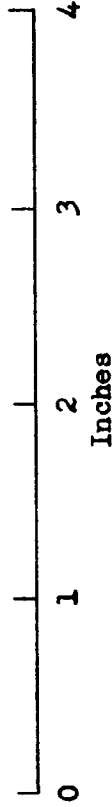


Fig. 19. Section through assembly of Mark 4 crystal gauge, type "S".

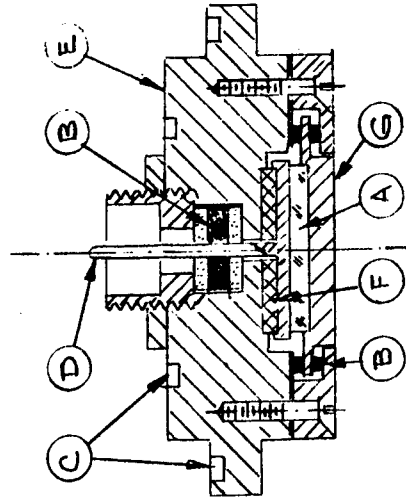


Fig. 20. Section through assembly of Mark 6 crystal gauge, type "R".

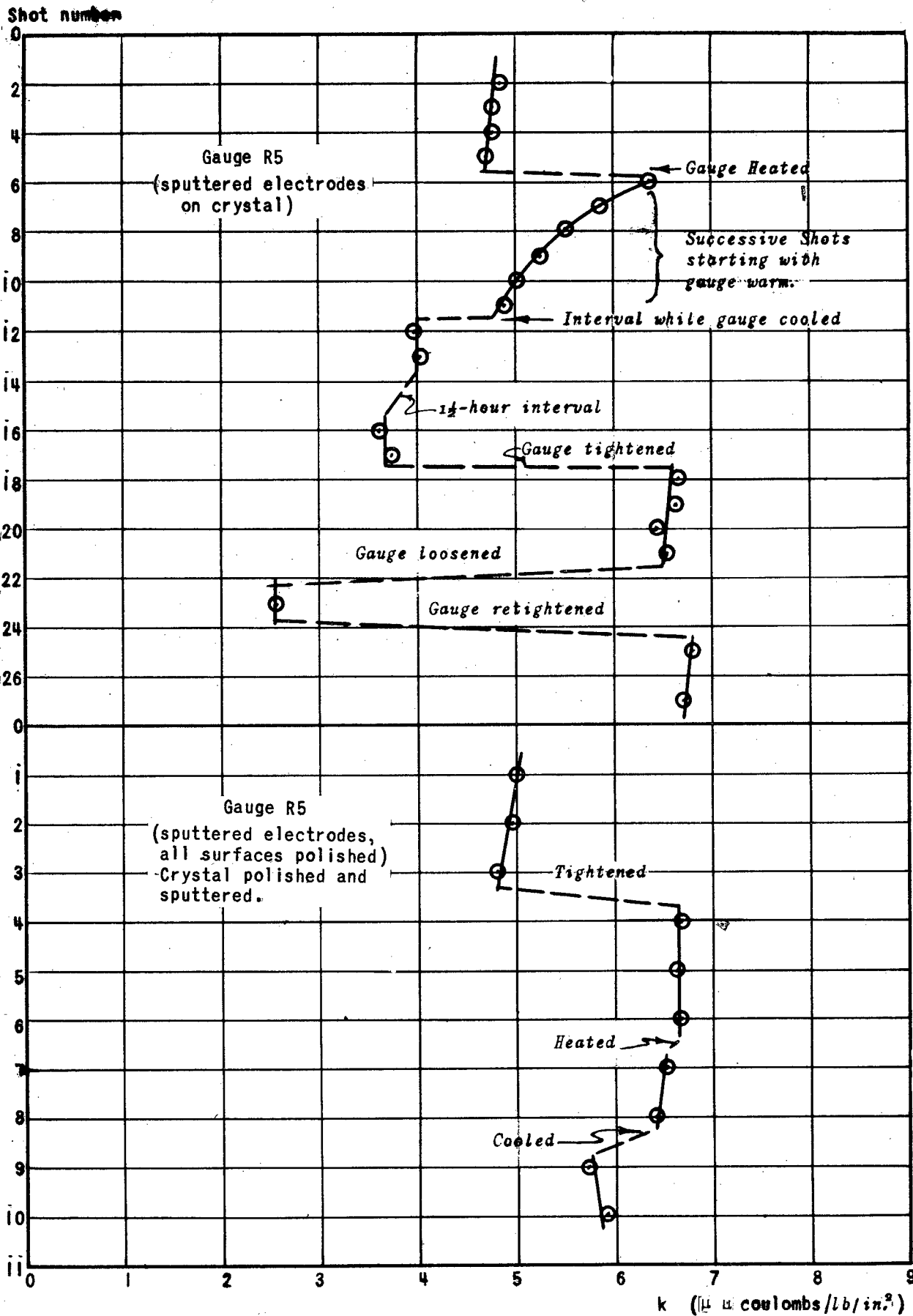


Fig. 2j. Gauge-constant variations.

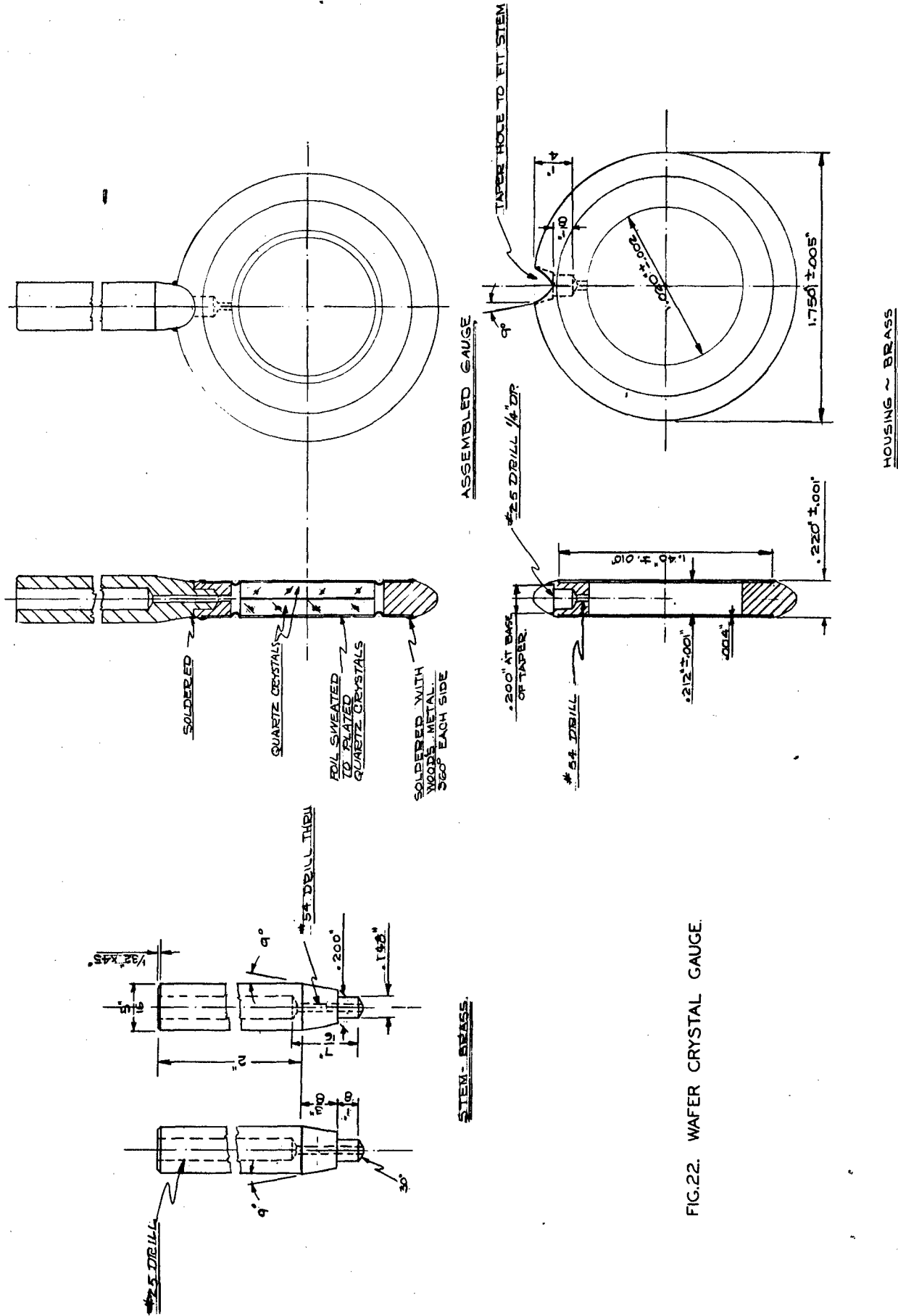


FIG. 22. WAFER CRYSTAL GAUGE.

X-cut quartz crystals is essentially constant over the range of temperatures and pressures involved,^{16/} it is clear that the variations observed must be due to the mounting of the quartz in the gauge rather than to the properties of the crystal itself. A suggested explanation is that the static pressure affects the contact between the quartz and the parts that serve as electrodes, and alters in some way the magnitude of the effective charge collected. A layer of 1-mil lead foil, at least, was always used on each face of the crystal to provide better mechanical contact, but this may not be sufficient. Experiments with polished crystals and electrodes and with sputtered or plated crystal surfaces showed very little consistent improvement. Other explanations, such as bending of the crystal from distortions of the case, have also been proposed, but the phenomenon is apparently quite complicated and no completely satisfactory explanation has been found.

(c) The wafer gauge. -- With the idea in mind of producing a quartz gauge that did not depend on a pressure contact between the crystal and the electrodes, experiments were begun on a design originally suggested by W. Bleakney. Since the d_{12} constant of quartz is equal to $-d_{11}$, equal pressures on the X- and Y-faces of a quartz crystal produce no net charge on the X-face. Thus the minimum housing required for a circular X-cut crystal is a guard ring to protect the edges of the crystal from exposure to pressure, while the X-faces are exposed. Through the courtesy of the R.C.A. Laboratories at Princeton, several crystals had been coated with a copper layer plated on a baked silver surface, which could be soldered with Wood's Metal without destroying the bond. A gauge design employing these crystals is shown in Fig. 22. This has been named the wafer gauge.

In assembling the gauges, the positive faces of two crystals were first tinned heavily with Wood's Metal, using very weak hydrochloric acid as a flux, and sweated together by heating on a hot plate to a temperature just above the melting point of the Wood's Metal, using a weight to force out the excess metal. The outer faces of the two crystal piles were then tinned and the edges of the crystals carefully cleaned by filing and rinsing with acetone or alcohol, followed by distilled water. Using Wood's Metal and a

^{16/} See, for example, A. Scheibe, Piezoelektrizität des Quarzes, (Dresden and Leipzig: T. Steinkopff, 1938); and A. Langevin, J. de Physique et le Radium (7) 7, 95 (1936).

cool iron, a length of No. 24 bare copper wire was then soldered to the exposed edge of the joint between the two crystals around the entire circumference and allowed to extend for about 4 in. to form a lead to the center electrode. A length of vinylite insulation was slipped over the extending wire and pushed down as close to the crystals as possible. The edges of the pile were then coated with Duco cement, to complete the insulation of the center conductor. Duco was chosen because it dries quickly and apparently stands heating to the temperature required during the remainder of the assembly of the gauge ($< 100^{\circ}\text{C}$). A coil varnish would perhaps have more satisfactory insulating properties, if sufficient time were allowed for it to dry without baking, since the crystals must be kept below the melting point of Wood's Metal at this stage.

The inner surfaces of the two copper diaphragms were then tinned with Wood's Metal and one was sweated onto the guard ring, to which the stem had already been fastened with ordinary solder. The amount of tinning on the diaphragms and the outer faces of the crystal is quite critical, since there must be enough to provide an all-over bond between diaphragm and crystal, yet not so much that drops squeeze out and fill the space between the crystal and the guard ring, shorting the gauge by making contact with the center electrode. The Duco covering helps prevent this. For the final assembly, the crystal pile is placed in the gauge with the lead wire threaded through the stem; the second diaphragm is put in place; and the whole gauge is put between two cylindrical blocks with flat ends having the same diameter as the diaphragms to insure all-over contact. A weight of about 25 lb is placed on the upper block. The whole assembly is then heated to a temperature slightly above the melting point of Wood's Metal (70° to 100°C) and then allowed to cool with the weight in place. An ohmmeter connected across the gauge terminals during this phase of the procedure will show whether the gauge becomes shorted during the heating.

The last step in the construction of the gauge consists of touching up the joint around the diaphragm with extra Wood's Metal applied with an iron to insure a complete seal, after which the excess is filed off and the gauge polished to a smooth contour. Photographs of gauges in the various stages of assembly are shown in Figs. 23, 24, and 25.

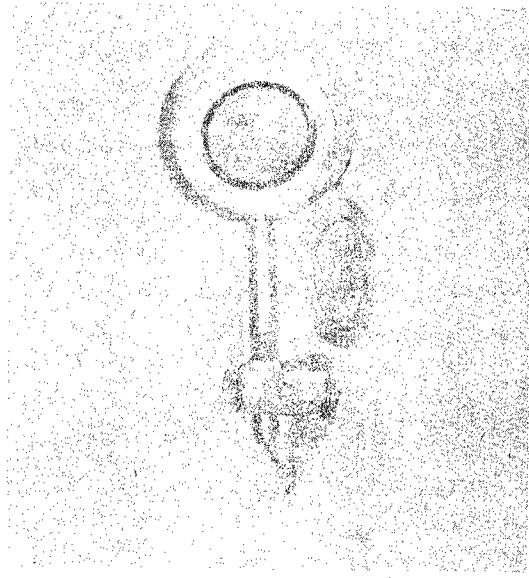


Fig. 24.

Fig. 23-25. Wave-gauge assembly.

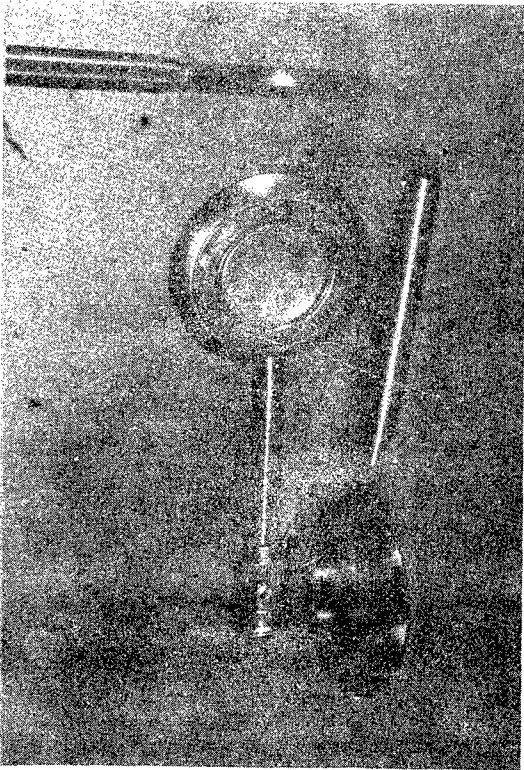


Fig. 23.

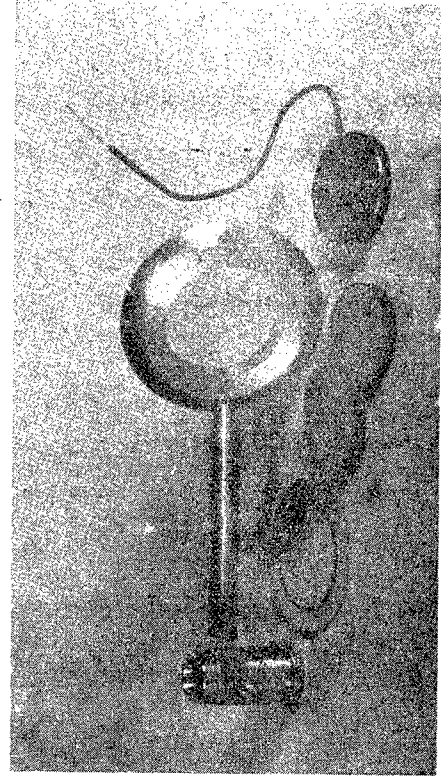


Fig. 25.

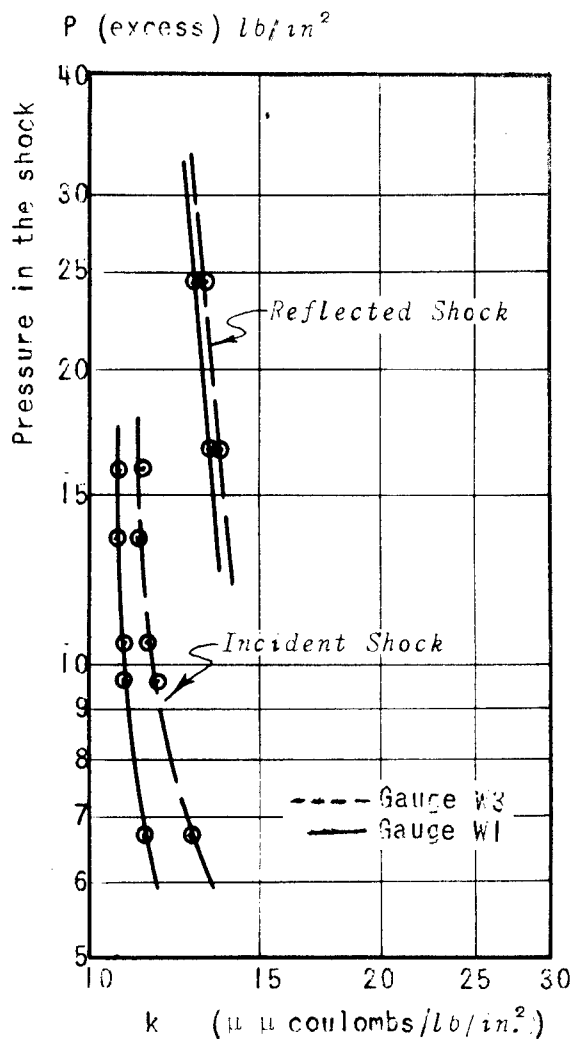


Fig. 26. Linearity test of two wafer gauges.

Tests in the shock tube of the first of these gauges assembled showed several faults. Several vibration frequencies were apparent, one of somewhat less than 1 kc/sec, and the others of the order of 5 to 15 kc/sec. The latter particularly depend on the alignment of the gauge relative to the incident shock, varying in amplitude from about 10 percent of the deflection amplitude when the gauge is placed accurately side-on, to about 50 percent for a gauge rotated 15° from the side-on position. A rotation of as little as 2° from the optimum alignment makes a noticeable difference in the amplitude of the vibrations.

The lowest frequency of vibration was thought to involve bending of the stem where it joined the gauge, since the first stem designed was much thinner at this point than the one shown in Fig. 22. The heavier stem reduced this trouble. When second and third gauges were made, care was taken in assembling the crystals to line up the optic (Z) axes of the crystals (which lie parallel to the X-faces) parallel to each other in one gauge, and at right angles in another. The gauge with the Z-axes parallel was found to be less subject to vibrations and to pressure on the supposedly insensitive parts of the case than the other gauges. While this is not a conclusive test, it is an indication that this orientation of the crystals may be preferable.

The crimp pressed into the diaphragms, partly to make it easier to center the crystals in assembling the gauges, was also found to be important in making the gauge insensitive to pressure on the edges of the ring. The crimp apparently helps isolate the crystals from shearing stresses produced by deformations of the guard ring. A gauge assembled with flat diaphragms proved to be very sensitive to tapping on the edge, as sensitive in some spots as on the faces themselves.

The second fault, observed in the first wafer gauge, was an upward slope in the top of the response curve when a flat-topped pressure wave was applied. This was found to be a pyroelectric effect, resulting from the heating of the thin copper diaphragm in the high-temperature region following the shock. A rough computation indicated that a temperature rise of 15 deg C at the surface of the crystal was possible even with a shock of only 3 or 4 lb/in². Expansion of the diaphragm would produce a tension along the Y-axis of the crystals which would add to the charge observed on the

X-faces. A sharp pulse could easily be observed by sweeping the gauge rapidly through a bunsen-burner flame. An insulating layer produced by dipping the gauge several times in rubber cement eliminated this effect satisfactorily. Later a coating of Bostik cement applied by dipping was also used, providing a much neater covering.

A series of measurements of gauge sensitivity as a function of shock pressure, using both direct and reflected shocks, was made in the same manner as will be described in Sec. 2 of this Part for tourmaline gauges. The results for two gauges are shown in Fig. 26. There is considerable scatter in these measurements, and any interpretation of the results must be made cautiously. It does appear, however, that the variation in gauge constant with pressure is more nearly the same for direct and reflected shocks than in the case of tourmaline gauges. Thus the gauges apparently have an inherent nonlinearity while the suggested nonlinearity due to the Bernoulli effect (see below) is much reduced, as would be expected since the wafer gauges are considerably better streamlined than are the tourmaline gauges.

One series of tests was made with the best wafer gauge that was constructed, to check variation of sensitivity with temperature. The gauge was calibrated with several shots at room temperature (about 26.4°C) and then immersed in a bath of melting ice for 8 min. It was then replaced in the tube and recalibrated as quickly as possible, a series of shots being taken at frequent intervals as the gauge returned to room temperature. These results are plotted in Fig. 27, where the ordinate is the ratio of gauge sensitivity k_t at time t to the sensitivity k_0 determined immediately before the gauge was cooled, plotted against time in minutes, counted from the removal of the gauge from the bath. It is apparent that the extreme changes in sensitivity with temperature observed in the "R" and "S" type gauges have been eliminated in the wafer gauge.

In other respects, the wafer gauge compares not unfavorably with the earlier quartz gauges, and while it has not been subjected to any field tests, it is felt that it at least offers a promising basis for further development.

2. Response of tourmaline gauges

Ten tourmaline gauges that gave good or fairly good records in the blast tube were calibrated over a range of temperatures between 10° and 45°C .

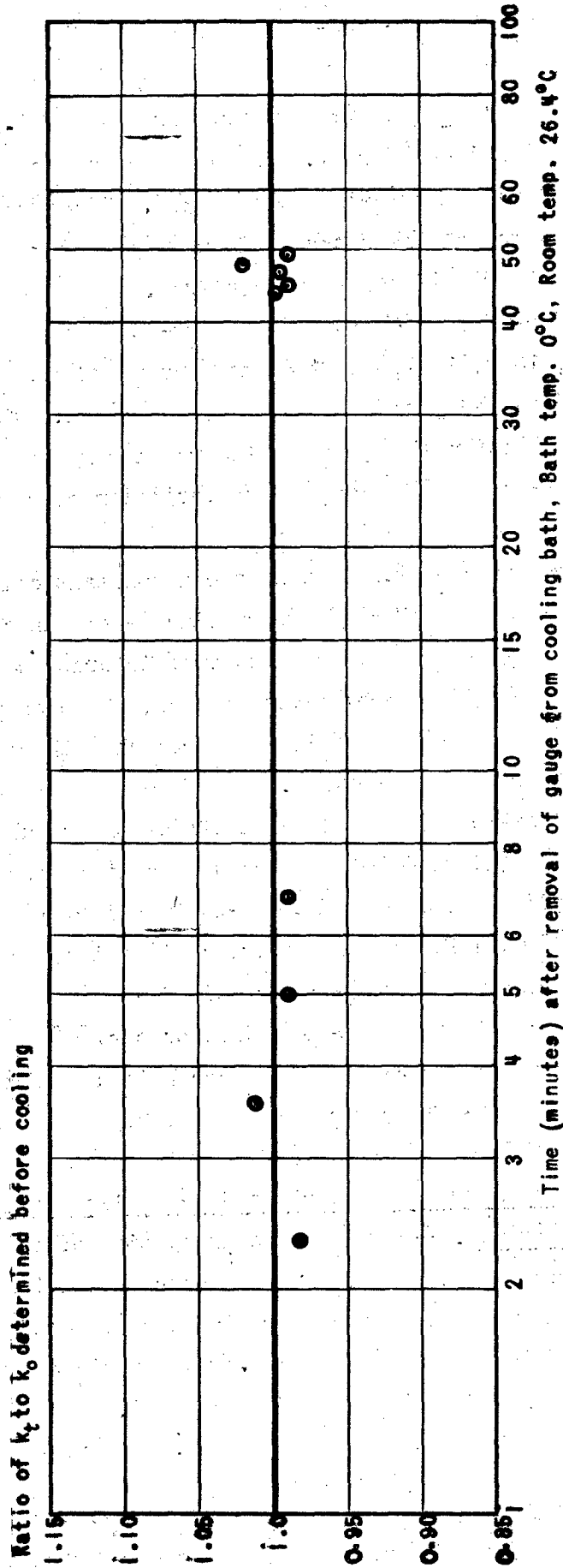


Fig. 27. Temperature effect on quartz wafer gauge.

Average changes in sensitivity k with temperature varied from 2.3 %/deg C to no change at all over the entire interval. In every case where a change occurred, the k decreased with increasing temperature. There was no correlation between the excellence of the records given by a gauge and the consistency of its calibration at different temperatures.

Four new tourmaline gauges of the central brass-tab design shown in Fig. 28 (gauges No. 973, 1000, 1001, and 1003 made by the Stanolind Oil and Gas Company) were calibrated at three different temperatures. The records from these gauges were exceptionally good and the results for the most part were quite consistent. There was no evidence of variation of gauge constant with temperature.

The fact that the gauges of newer design gave a constant calibration suggests that the effect of temperature on tourmaline gauges is characteristic only of old and much used ones, or of gauges of inferior design or construction. However, of the older tourmaline gauges, those showing a temperature effect were in no way distinguishable from the others except by actual calibration at different temperatures.

The influence of temperature on gauges will affect the results of a field program in two ways. (i) There will be random scatter in recorded pressures throughout the program, due to shot-to-shot variations of temperature. (ii) Since it is improbable that the gauge calibration for a program would be done at exactly the average temperature of the pressure measurements, there will be an error in the best-fit curve or curves for the program. The magnitude of this latter systematic error will depend on the difference between the calibration temperature and the average temperature for the pressure measurements.

(a) Character of records given by quartz and tourmaline gauges at high incident and reflected pressures. -- After the construction of the present tube (Figs. 1 to 5), which can take much higher pressures than the original design, the first experiments to be performed were tests of both quartz and tourmaline gauges over a wide range of pressures. Both incident and reflected pressures were used, the incident pressures ranging from 3 to 20 lb/in² and the reflected pressures from 4 to 40 lb/in².

A great difference was noticed in the behavior of quartz gauges in the old and new tubes. In the old tube it was necessary to mount the gauge as

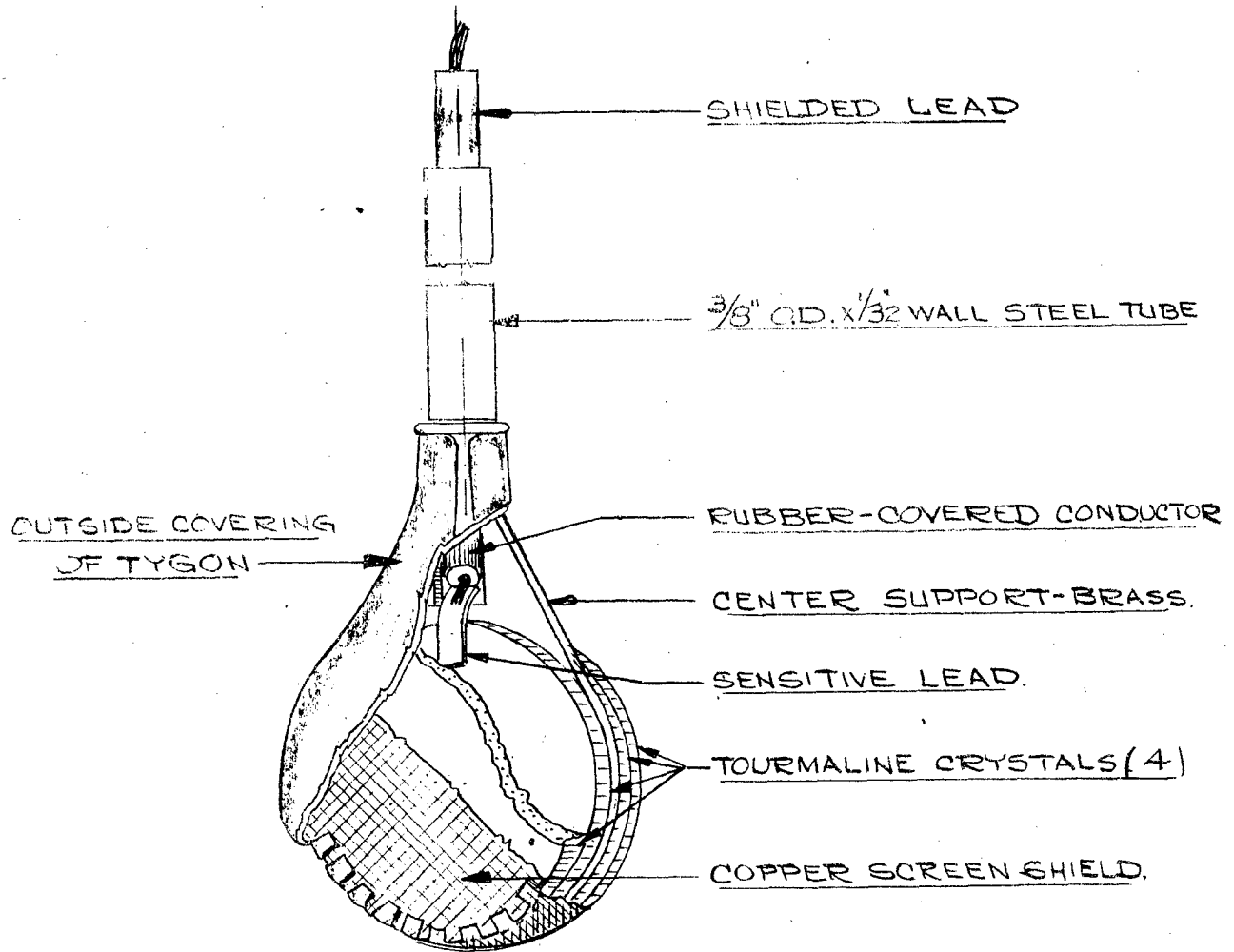
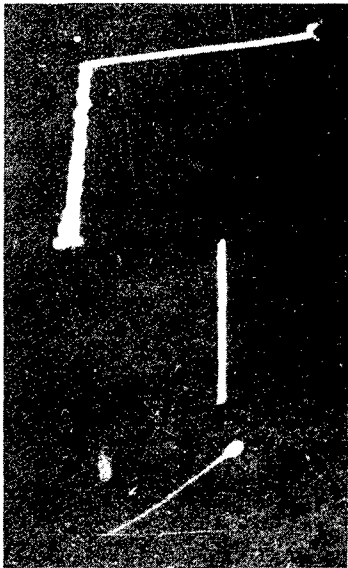


Fig. 28. Cutaway view of tourmaline gauge construction, central brass-tab gauge.

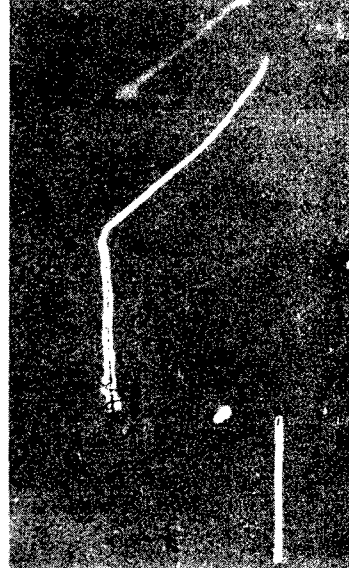


P = 3.30 lb/in.²
Fig. 29.

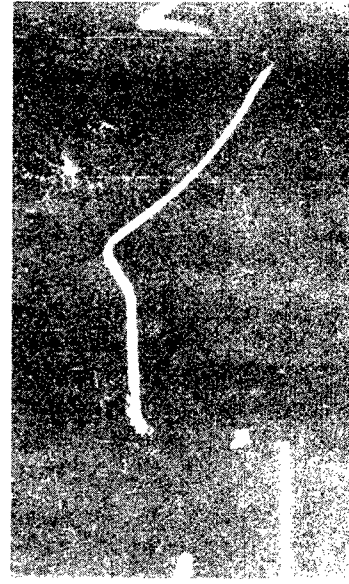


P = 19.7 lb/in.²
Fig. 30.

Figs. 29-30. Typical tourmaline gauge traces, incident shocks.



P = 25.1 lb/in.²
Fig. 31.



P = 38.0 lb/in.²
Fig. 32.

Figs. 31-32. Typical tourmaline gauge traces, reflected shocks.

loosely as possible in the tube to obtain traces that were at all satisfactory. In the new tube, which is much more rigid and more massive (because of the solid piece inserted to give the noncircular cross section), almost vibrationless records were obtained by clamping the gauge rigidly to the tube.

The older tourmaline gauges gave very irregular patterns when subjected to high incident pressures. However, the same gauges gave excellent records for much higher reflected pressures. This would indicate that the irregular patterns given by tourmaline gauges are due, not to the high pressures but, perhaps, to the high particle velocity since the particle velocity behind the incident shocks increases with shock pressure while the particle velocity behind reflected shocks is zero for all pressures.

Gauges of the new central brass-tab design (Fig. 28) give much better records for incident pressures than did the earlier gauges. This is probably because of the added stiffness in the neck of the gauge. These gauges give almost perfect records for incident shocks below 10 lb/in² excess pressure. For incident shocks between 10 and 15 lb/in² the records are quite readable but slant downward. Above 15 lb/in² the records become more slanted but are generally usable. At or around 20 lb/in² in the incident shock it is almost impossible to obtain satisfactory records. In all cases the oscillograms are measured to the intersection of the initial rise with a line through the mean of the gauge vibrations (see Figs. 29, 30, 31, and 32). The hump at the end of the stop in Fig. 32 is a reflection from the gas boundary.

Both quartz and tourmaline gauges gave steps with somewhat rounded corners for high reflected pressures. The amount of rounding increased with pressure. No satisfactory explanation of this effect has yet been found. It was thought that the rounding might be due to deformation of the $\frac{1}{4}$ -in. brass end plate, which would cause a temporary relief of pressure at the end of the tube. However, this explanation was refuted when the same rounding was observed with a 5-in. steel end plate.

(b) Response as a function of pressure level. -- Four of the new brass-tab design gauges were calibrated over a range of both incident and reflected pressures. Three shots were taken on each gauge at each pressure. The averages of the three determinations of k are plotted against pressure in

Figs. 33, 34, 35, and 36. The results show that k decreases with pressure when incident pressures are used but is almost constant with pressure when reflected pressures are used.

Again the effect of particle velocity is suggested. The pressure that is used in computing the gauge constant is determined from the chamber pressure and from a plot of shock pressure versus chamber pressure based on velocity measurements. During the velocity measurements no gauges are in the tube. Thus the pressures used in computing k 's are the pressures that would be produced if no gauges were in the tube. However, the presence of the tourmaline gauge projecting into the tube will distort the streamlines and cause a local variation in pressure at the gauge. Thus the pressure actually acting on the gauge is not the pressure that would act at the same point in the tube if no gauge were there and it is the latter pressure that is determined in velocity measurements and used in computing gauge constants.

Since the presence of the gauge will increase the local particle velocity, according to Bernoulli's theorem the pressure on the gauge will decrease. This will make the gauge appear to be less sensitive at higher pressures, which is actually what is observed.^{17/}

For reflected pressures there is no particle velocity, and no variation in gauge sensitivity would be expected.

The foregoing explanation in terms of distortion of streamlines and Bernoulli effect is admittedly speculative but it accounts well for all the known facts, and in any case it seems very probable that the response of a gauge that projects into the tube is significantly affected by particle velocity.

^{17/} These results are confirmed by blast-tube results at the Underwater Explosives Research Laboratory (U.E.R.L.), "Characteristics of air-blast gauges: Response as a function of pressure level," by A. B. Arons, C. W. Tait, G. K. Fraenkel, and K. M. Doane, included in AES-3 (OSRD-4875). Air-blast experiments by U.E.R.L. indicate that the response of the gauges to shock waves in the tube is substantially the same as to the "free-air" shock wave produced by high explosives. See "Characteristics of air-blast gauges, II: Response as a function of pressure level," by C. W. Tait and W. D. Kennedy, included in AES-11 (OSRD-5271). A theoretical treatment of this problem is presented in "On the estimation of perturbations due to flow around blast gauges," prepared for the Applied Mathematics Panel, National Defense Research Committee, by the Applied Mathematics Group, New York University.

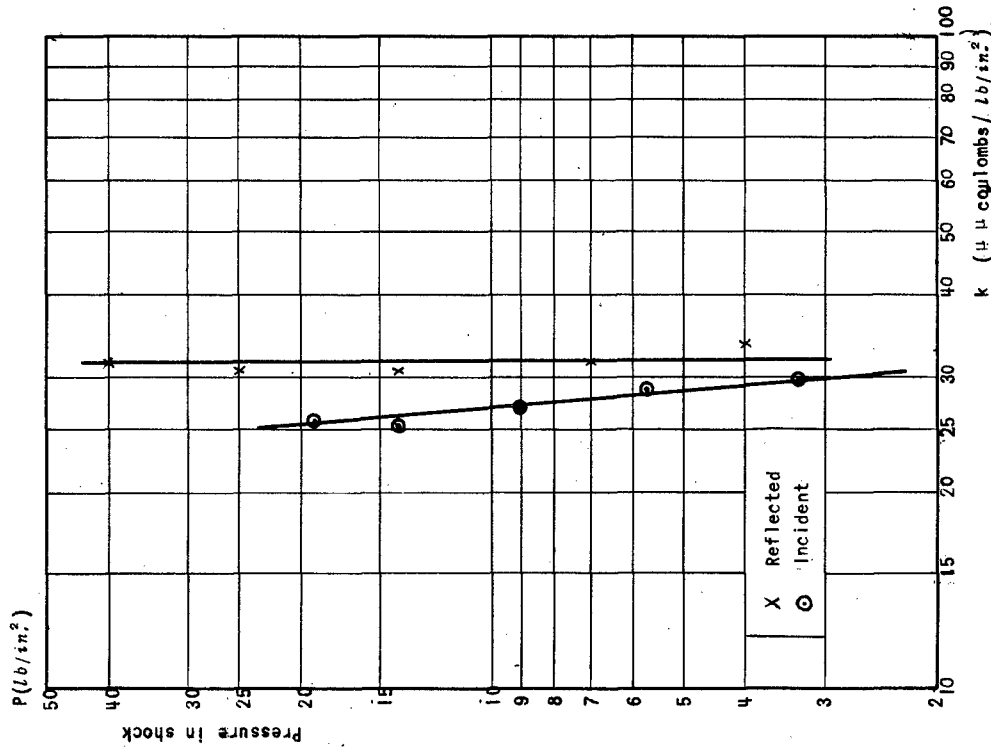


Fig. 34. Linearity test - Gauge 1000.

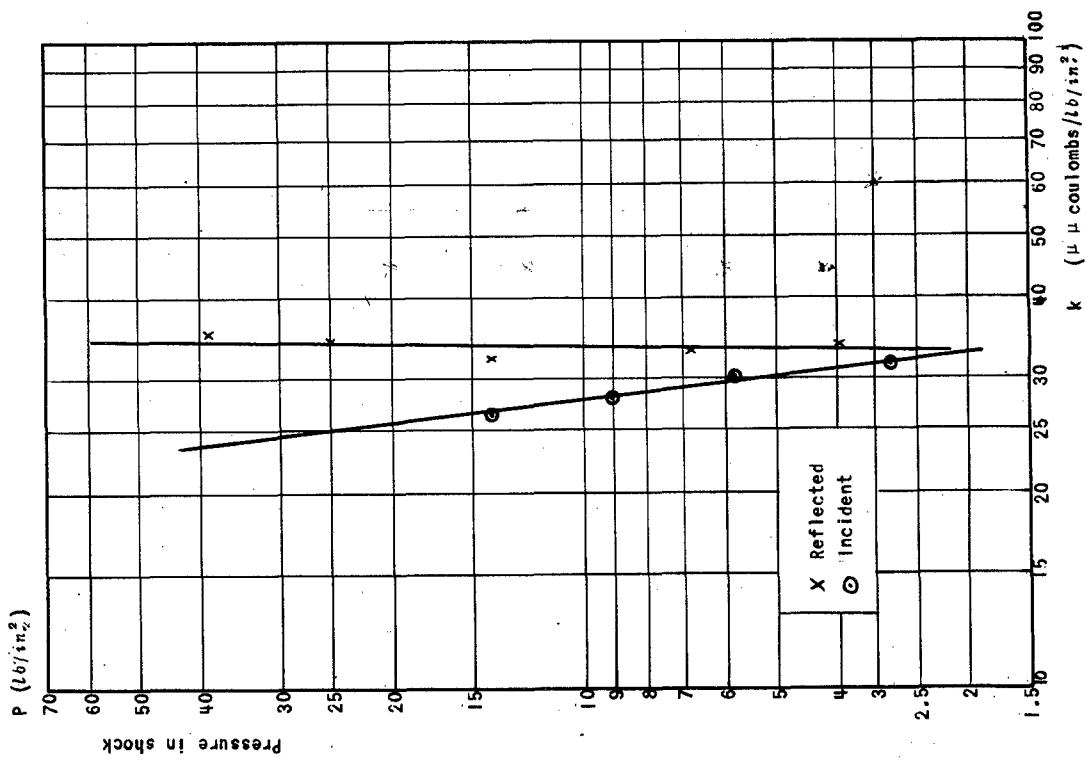


Fig. 33. Linearity test - Gauge 973.

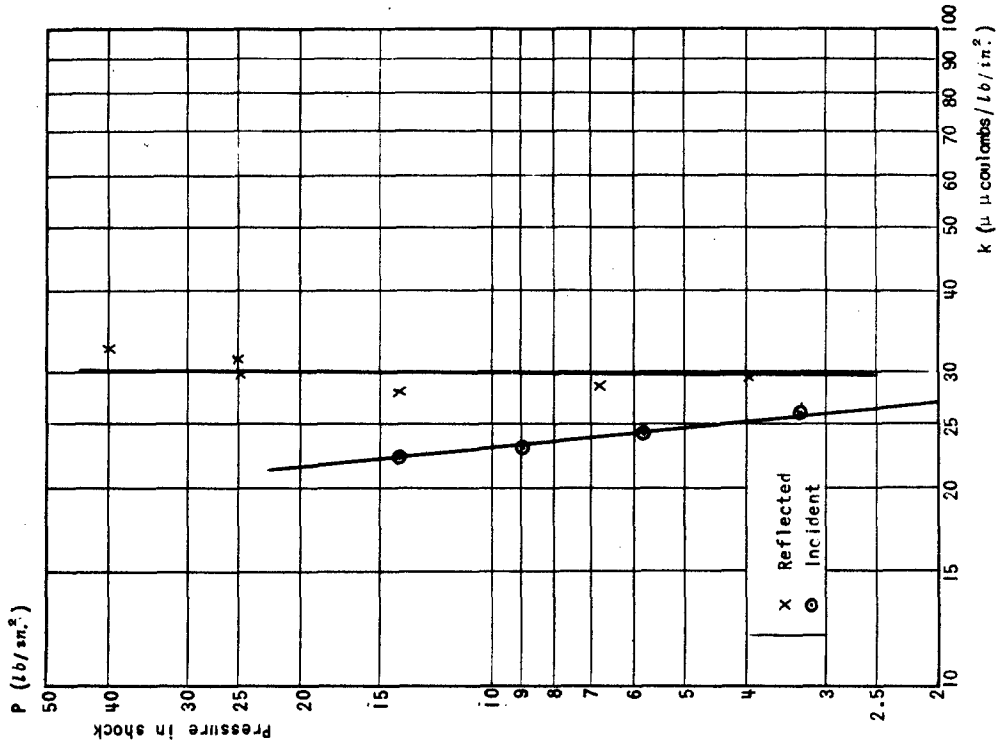


Fig. 36. Linearity test - Gauge 1003.

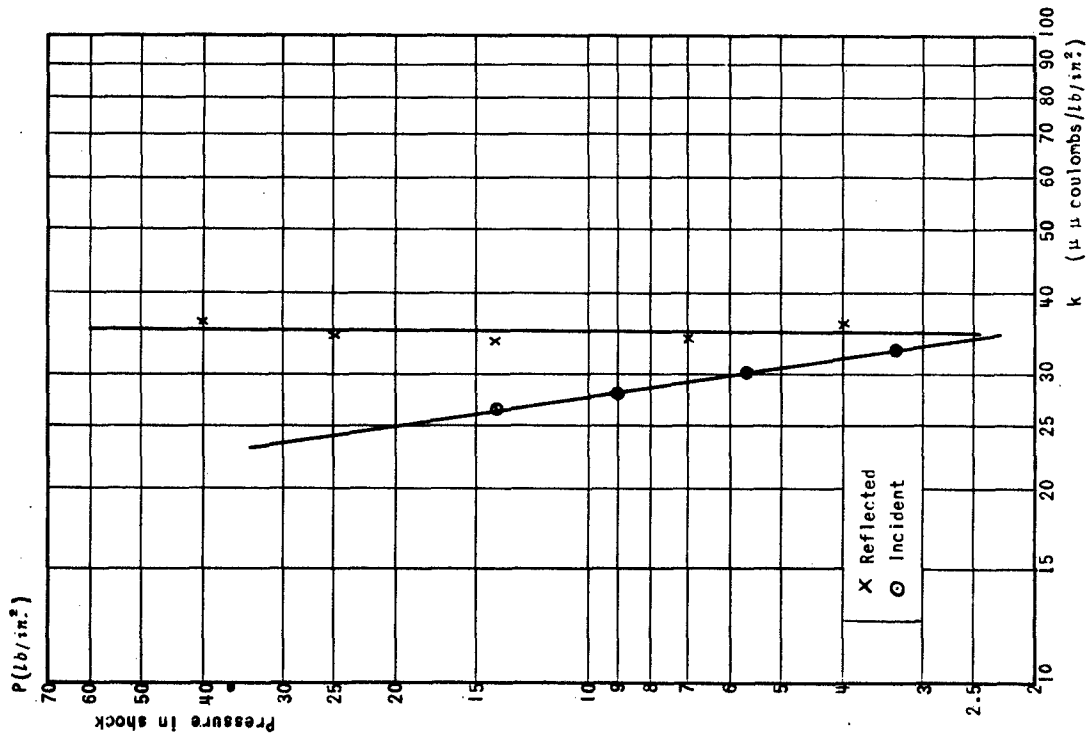


Fig. 35. Linearity test - Gauge 1001.

This conclusion is supported by tests of a tourmaline gauge that is mounted flush with the tube wall and therefore does not disturb the shock wave. The results of tests of this gauge over a range of incident and reflected pressures are plotted in Fig. 37. The agreement between the points obtained using reflected pressures and the points using incident pressures, and the lack of dependence of both sets of points on pressure level indicate the consistency that can be obtained when gauges are not subjected to any normal components of particle velocity.

3. Electronic apparatus

The essential apparatus contained in the present single-sweep equipment used for measuring transient pressures is shown in Fig. 36 and consists of the following pieces (numbered as in Fig. 38):

1. Timing oscillator
2. Calibration unit and distribution panel
3. A four-channel pre-amplifier
4. Four "modified" DuMont 175A cathode-ray oscillographs
5. Four camera boxes
6. Power supply for pre-amplifiers
7. The trigger circuit for beam intensification and sweep circuit
8. Initiating trigger circuit and circuit for delaying the calibrating relay
9. Firing circuit
10. Intercommunication set
11. Motor generator for converting a.c. to d.c. for the camera solenoids

Most of these or similar pieces have been described in a previous report,^{18/} hence only radical changes in each will be discussed in detail.

(a) Pre-amplifier section. -- The pre-amplifier section (see Fig. 39) consists of two amplifier stages preceded by cathode followers directly coupled to the amplifier grids, a cathode-follower output stage, and a phase-inverter stage for inverse feedback. The advantages of cathode followers between amplifier stages are^{19/}

^{18/} The measurement of transient stress, displacement and pressure, by C. W. Lamson, NDRC Report A-73 (OSRD-756).

^{19/} Ultra-high-frequency techniques, by J. G. Brainard (Van Nostrand, 1942) pp. 221-222.

- (a) a high input resistance to the amplifier allowing the use of larger grid-leak resistors to obtain larger time constants,
- (b) a low input capacity allowing the use of larger amplifier plate loads for the same frequency response.

The advantages of the feedback circuit are^{20/}

- (a) a greater frequency range,
- (b) a greater stability of amplification,
- (c) a smaller amplitude distortion.

Measurements made with the gain control set at a maximum (minimum feedback) indicate a frequency response that is essentially flat in the middle range, falling off 3 db (approximately 30 percent) at 0.1 cycle/sec at the low end and 3 db at 150 kc/sec at the high, with a gain of 48 db (approximately 250 times) and a maximum distortionless output of about 2 v peak in either direction. An attenuator with approximately 2 db per step is made by varying the inverse feedback. It is thus frequency-discriminating, the worst response being that described.

There are some disadvantages to such a wide frequency band, namely, increased noise (tube, resistor, and microphonic), greater drift, and a longer time to come to equilibrium after the disturbance. Tube and resistor noise were reduced to a minimum by carefully selecting the tubes and resistors for the first stage. Microphonics were reduced by using specially constructed shock-mounts for this stage. Drift was reduced considerably by using a well-regulated power supply (see Fig. 40) and by using a line-regulating transformer.^{21/} The power supply was constructed with four separate regulators in anticipation of power supply "crosstalk" between channels, but this was later found to be unnecessary. It was found a wise measure to wait about 30 sec after each shot and about 2 or 3 min after a "shunting condenser" [see Fig. 41 and Sec. 3(c)] was changed to make certain the amplifier had returned to equilibrium.

(b) Vertical-axis amplifiers. -- Because of time constant and voltage-linearity considerations it was found necessary to revise slightly (see Fig. 42) the vertical-axis amplifiers in the DuMont 175A cathode-ray oscilloscopes. After this revision, the oscilloscopes were used almost continuously from

^{20/} Ref. 19, pp. 104-113.

^{21/} 115-v, 2-kw; constructed by Raytheon Mfg. Co.

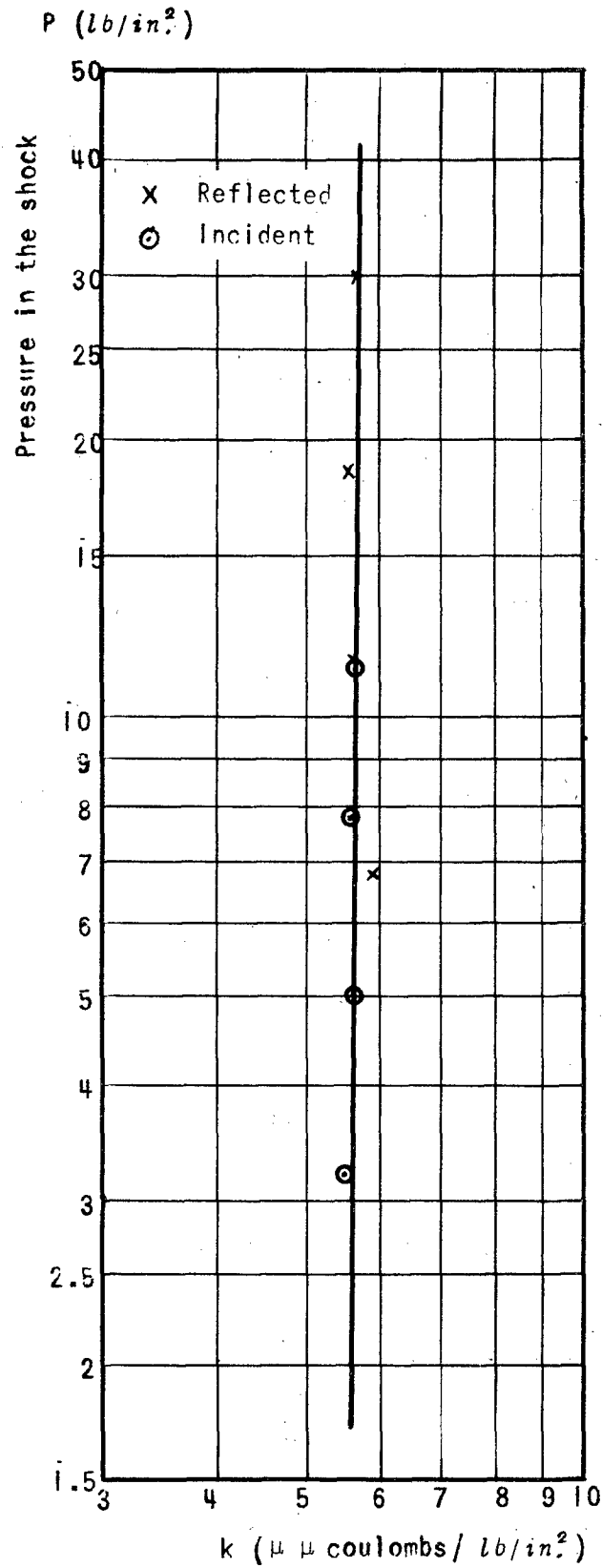
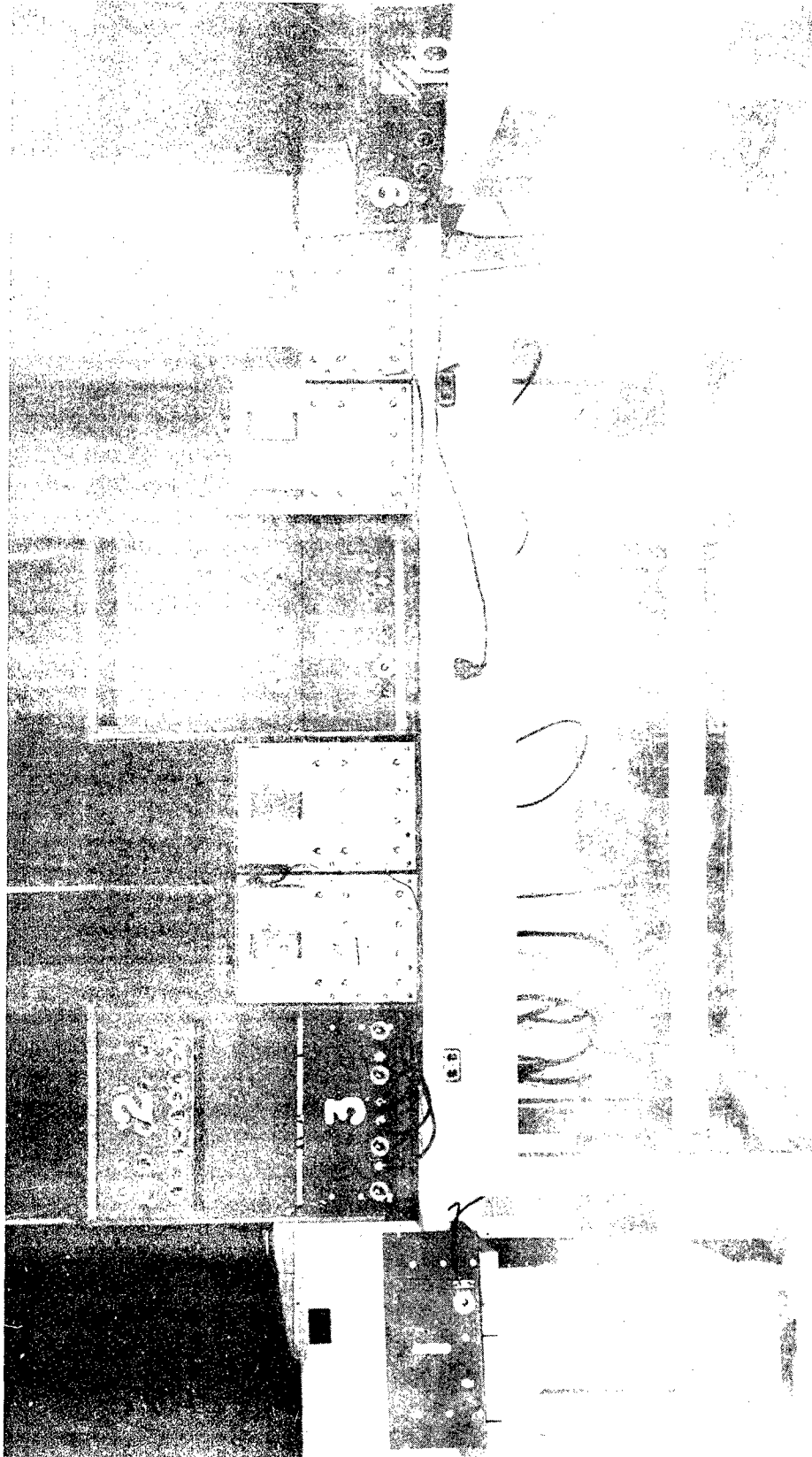


Fig. 37. Linearity test of flush tourmaline gauge 938.



- | | |
|--|---|
| 1. Timing oscillator | 7. Beam trigger and sweep circuit |
| 2. Calibration unit and distribution panel | 8. Initiating trigger circuit and delay for calibrating relay |
| 3. Four-channel pre-amplifier | 9. Firing circuit |
| 4. Transient oscillograph | 10. Intercommunication set |
| 5. Camera box | 11. D-c motor-generator |
| 6. Power supply for pre-amplifier | |

Fig. 38. Gauge recording station.

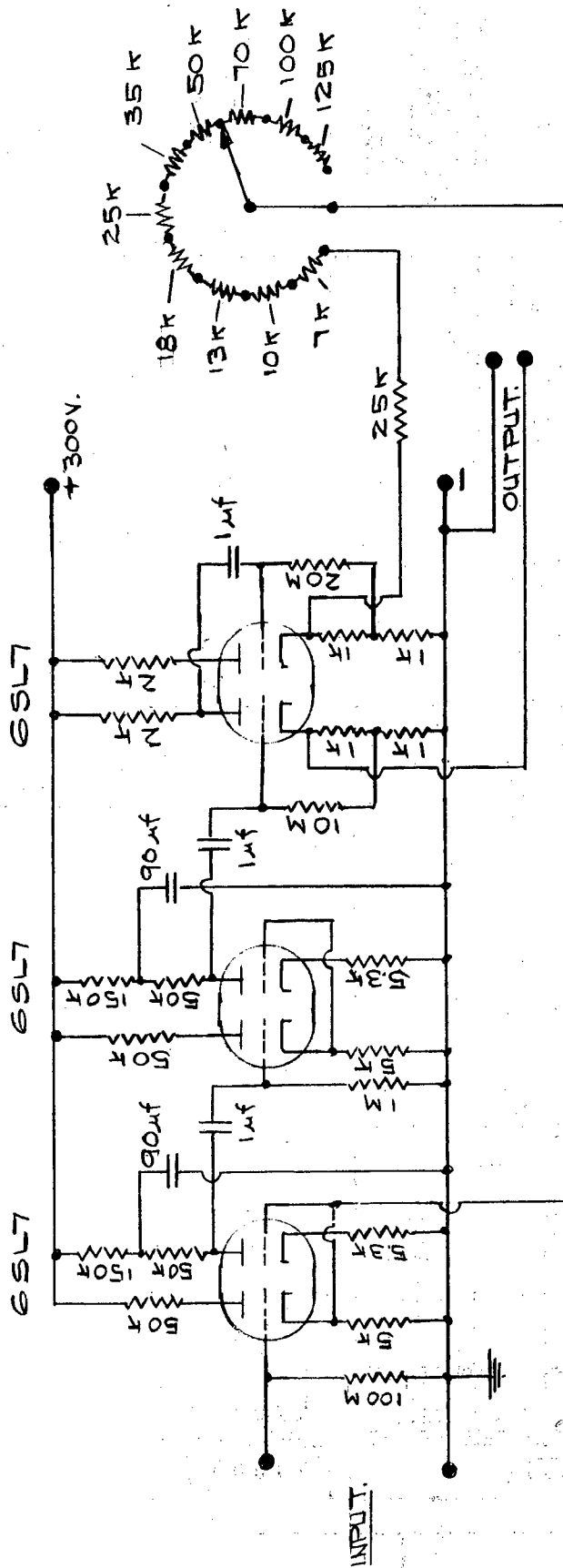


Fig. 39. One channel of a 4-channel amplifier.

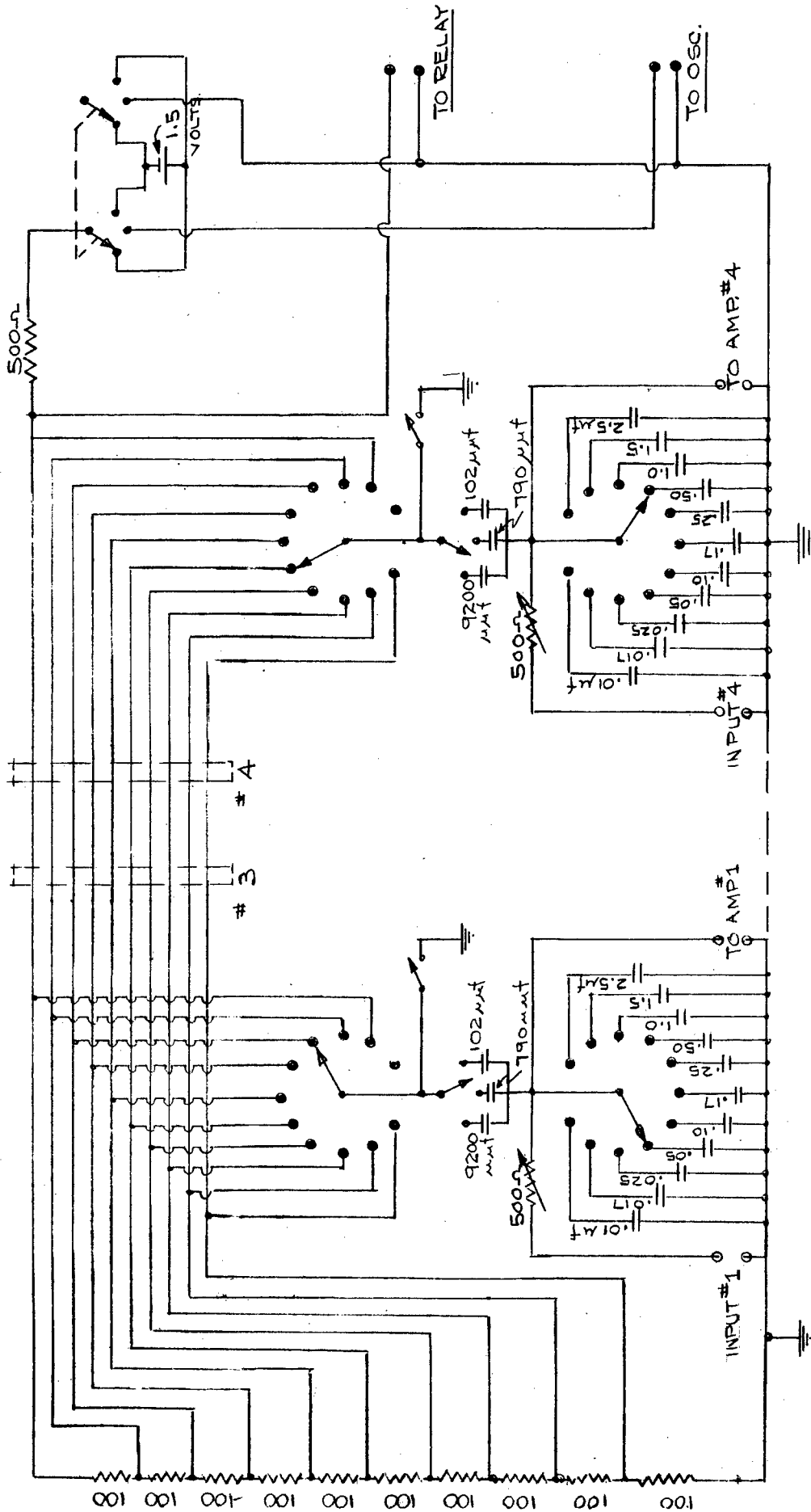


Fig. 41. Calibration and distribution panel for 4-channel single-sweep apparatus.

December 1944 until the present time. The circuit indicated in Fig. 42 has a time constant of 0.5 sec (down 3 db at 0.3 cycle/sec) and is down 3 db at about 150 kc/sec at the high end. It is linear within ± 1 percent over the deflection of $1\frac{1}{2}$ in. on either side of the center of the cathode-ray tube and within ± 5 percent over 2.3 in. This is at 20°C, but at higher temperatures (35°C) greater distortion was observed. Hence as long as the deflection was kept to less than 1.5 in. at normal temperatures, no error in measurements due to amplifier nonlinearity occurred. Used with the pre-amplifier that has been described, at the maximum gain setting there is an input voltage sensitivity of 90 μ v/in., a noise level of about 0.1 in. (on the oscilloscope), and an over-all time constant of about 0.4 sec and a high-frequency response (down 3 db) of about 100 kc/sec. The Z-axis was also modified in order that its time constant be comparable with the V-axis. Otherwise it is essentially the same as the original DuMont circuit.

(c) Calibration unit. -- The calibration unit (Fig. 41) consists of approximately the same circuit as that discussed in the report on the Princeton mobile oscillographic laboratory.^{22/} The standard condensers are arranged in 30 steps to give from 100 to 10,000 $\mu\mu$ coulombs by using 3 capacity steps and a voltage divider of 10 steps. This charge is placed across shunt-capacities of from 0.01 μ f to 2.5 μ f in logarithmically increasing steps of approximately a 2:1 ratio per step. Potentiometers (500-ohm) are placed in series with the line to compensate for its inductance. The charge is put suddenly on the condensers by opening a relay which short-circuits the applied voltage. This relay is incorporated in the "initiating trigger circuit" (Fig. 43) with a suitable circuit to delay its operation. These circuits, or similar ones, are described in a previous report on this equipment.^{22/}

(d) Trigger circuit. -- The trigger circuit for intensifying the oscilloscope beam during the sweep and the sweep circuit itself (see Fig. 44) are also quite similar to the original circuits described in an earlier report.^{22/} The sweep circuit was modified slightly by discharging the condenser through a pentode in which, as is well known, the plate current is essentially

^{22/} Mobile oscillographic laboratory, by C. W. Lampson and W. Bleakney, NDRC Report A-307 (OSRD-4570).

independent of plate voltage. This gives a much more linear sweep, which was measured to be linear within 1 percent over 2 in. of the oscilloscope screen.

(e) Timing oscillator. -- Since the early sine-wave calibration system^{22/} was abandoned, it was found convenient to use a different timing oscillator. A fixed frequency standard giving frequencies of either 1000 or 200 cycle/sec was built (see Fig. 45), and since sine waves were no longer necessary a "pip-circuit" synchronized with the oscillator was incorporated which gave small pulses of approximately 0.1-msec duration. A conventional transitron oscillator circuit was used and, although employing only an ordinary tuned circuit, it was found to give a constant frequency within 0.1 percent over all the temperature range normally found in the laboratory.

(f) Camera boxes. -- In order to photograph the oscillograph traces, four camera boxes were constructed (see Fig. 38) using Foth-Derby cameras with f:2.5 lenses and 127 Super XX film. The shutters of these cameras were operated by solenoids, all on the same d-c source, a motor-generator unit.

(g) Firing circuit. -- A firing circuit (Fig. 46) is used in conjunction with the single-sweep apparatus when measuring pressures produced by electrically exploded charges. It consists merely of two relays with appropriate delay circuits; one, to initiate the sweep, and the other, discharging a 500- μ f condenser (charged to approximately 50 v) through the fuze of the detonator. Either relay can be delayed as much as 50 msec and would repeat to better than 1 msec. It was discovered, however, that a variation of as much as 3 msec in the time of detonation of the charge could be recorded because of variation in construction of the various blasting caps used.

(h) Intercommunication system. -- An intercommunication system was used whenever measurements in the field were made, to coordinate work in the field with that in the laboratory.

4. Other equipment

In addition to the blast tube and electronic apparatus, it was found expedient to use two additional pieces of equipment that are deemed important enough to describe briefly here.

(a) The film-reading box. -- To facilitate the reduction and analysis of oscillograph records, a special film-reading box was designed to enlarge

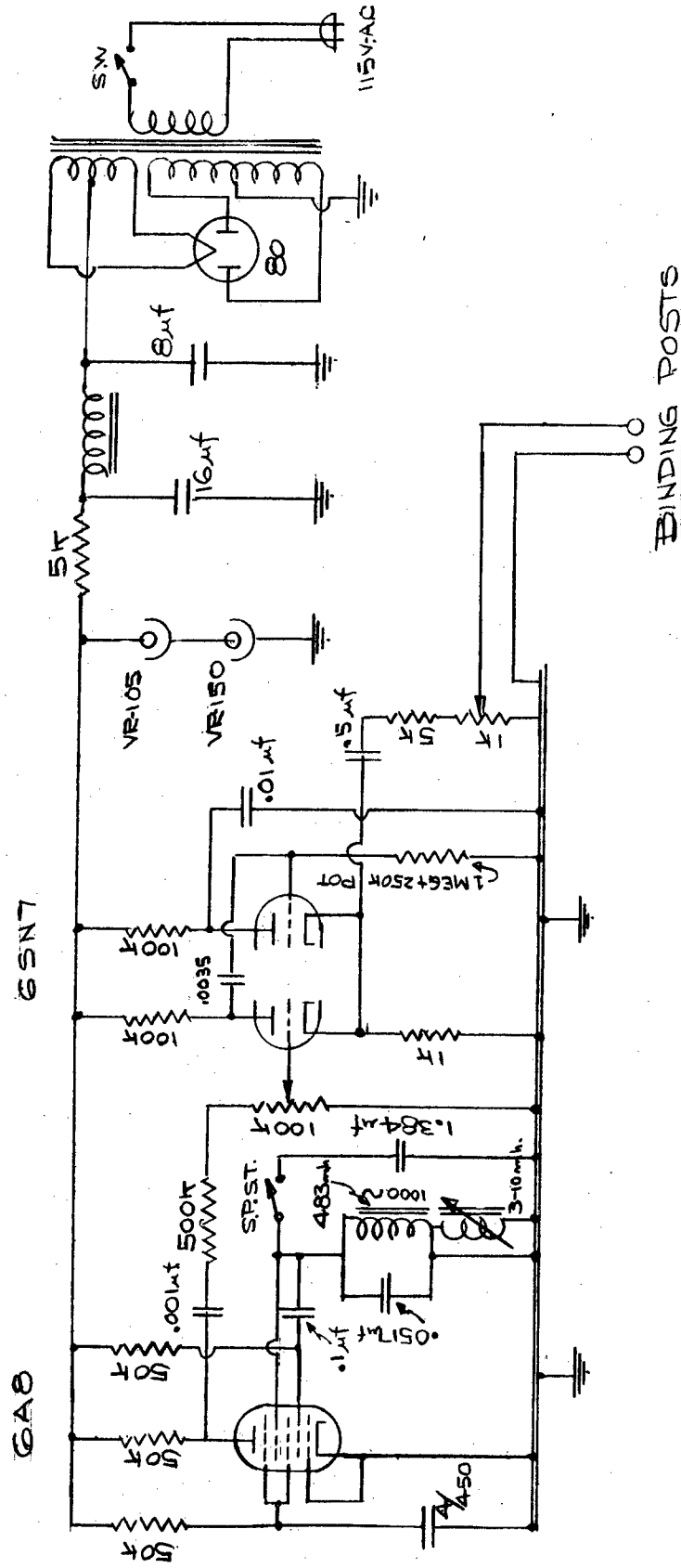
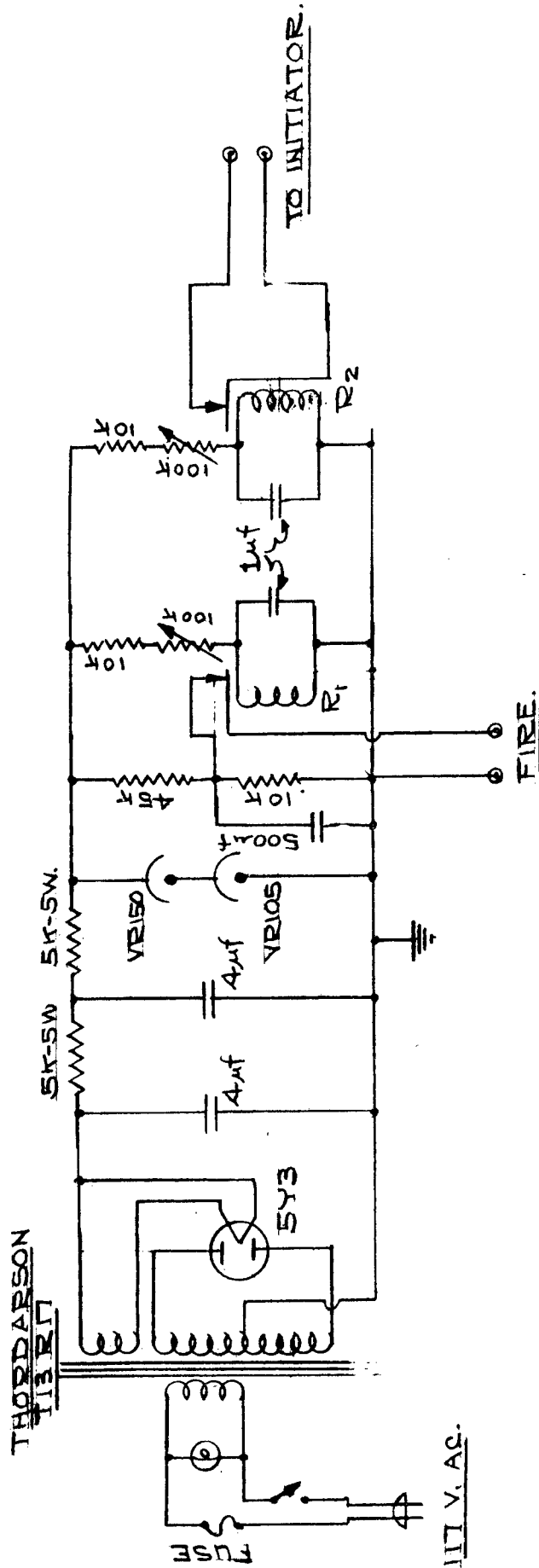
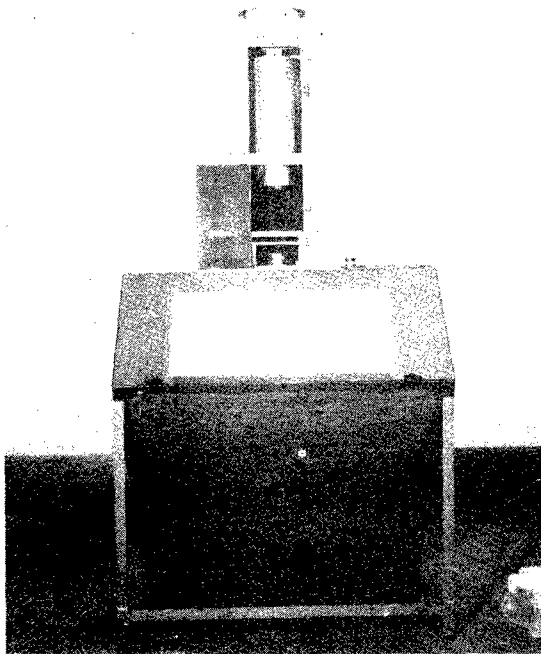


Fig. 45. Timing oscillator for single-sweep apparatus.

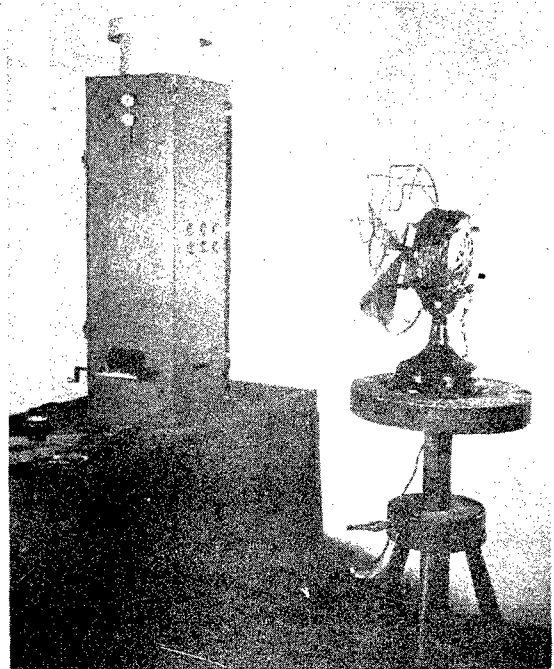


R₁ & R₂ = ADVANCE RELAY
TYPE 361 10,000-Ω
(NORMALLY OPEN)

Fig. 46. Firing circuit for use with single-sweep apparatus.



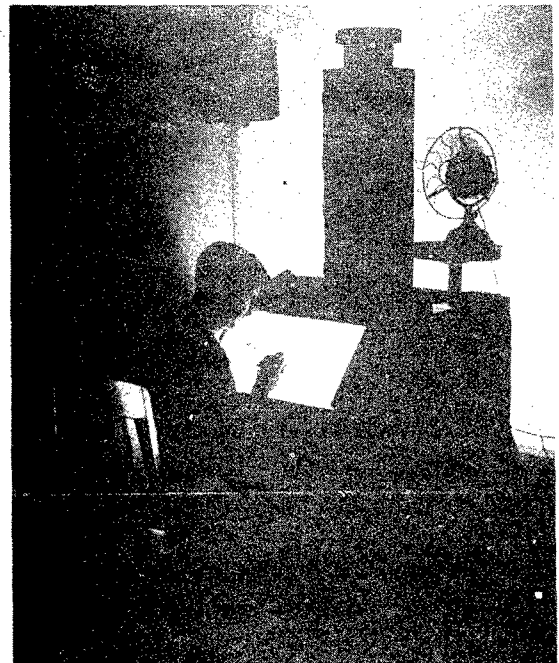
(a) Front view



(b) Side view.



(c) Interior view



(d) Projector in use

Fig. 47. Film-reading box.

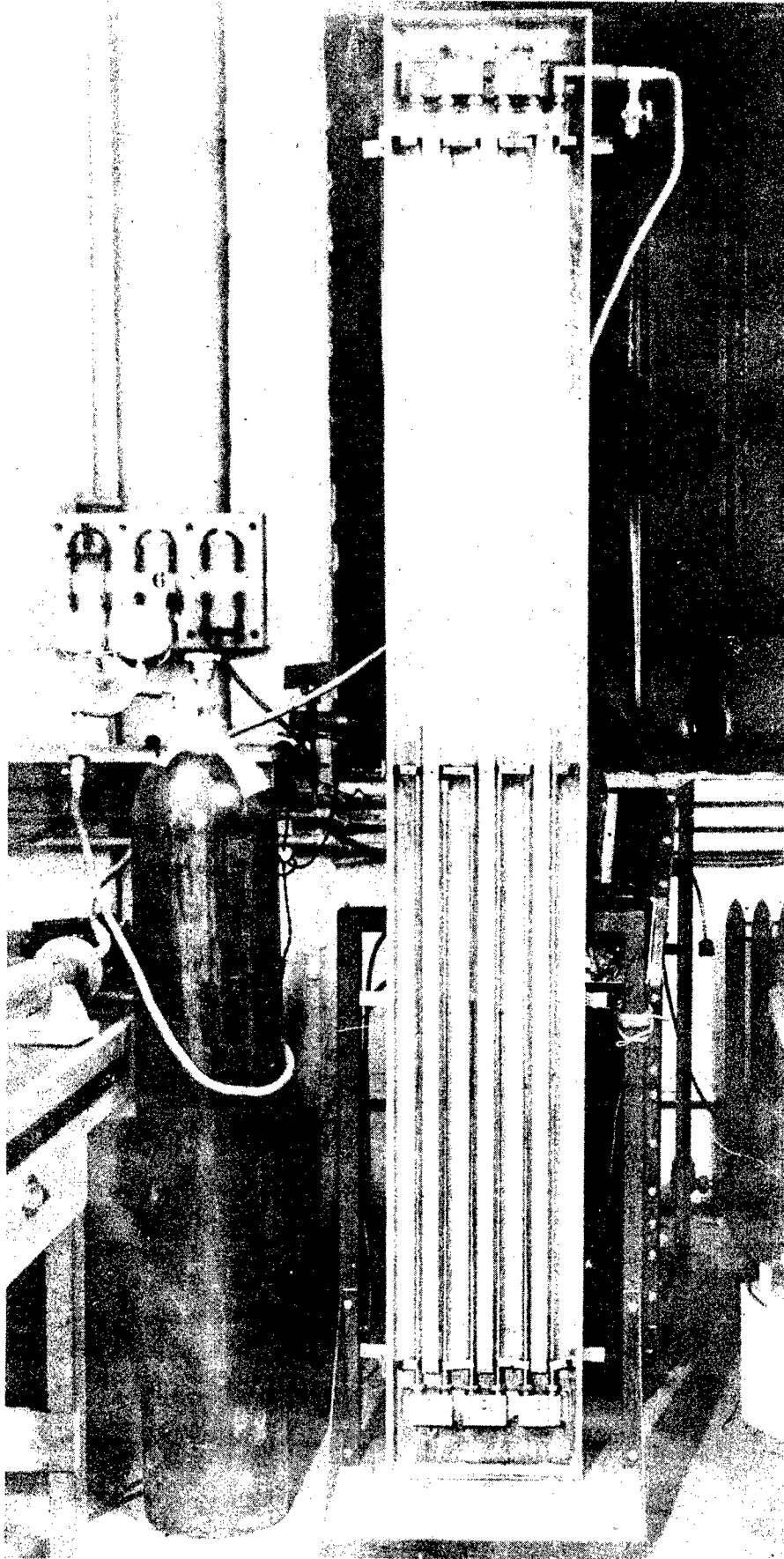


Fig. 48. Multiple manometer.

oscillograms originally photographed on 35-mm and 127 Super XX film. Enlargements of 7.8 times, 12.6 times, and 23.1 times were effected by the choice of the proper enlarging lens. Essentially the optical arrangement consists of a No. 2 photo-flood lamp as the light source, a pair of condensing lenses, film holder and film, enlarging lens, reflecting mirror, and opal screen upon which the oscillogram is projected.

Measurements may be made directly from the opal screen image or, if permanent records are desired, from suitable tracing material such as "Kodatrace" upon which a copy of the oscillogram is drawn. The latter is the method employed when impulse data are desired and a convenient size is needed for accurate planimeter measurements. (The impulse, of course, is proportional to the area under the force-time record.) Figure 47 shows front, side, and interior of the film-reading box used at Princeton from September 1944 until the present time and also shows the same box in actual use.

(b) The multiple manometer. -- For accurate measurements of static pressures, it was found necessary to use manometers. To prevent the necessity for an exceedingly tall manometer to measure high pressures, a so-called "multiple manometer" was used. The Princeton design consisted of three mercury manometers connected in series, the first to the second and the second to the third, and coupled by distilled water. This gives approximately one-third the deflection produced in a single mercury manometer for an equivalent pressure. The manometer, as shown in Fig. 48, measures pressures up to 90 lb/in² to within 0.05 lb/in².